Applications of Acid–Base Blend Concepts to Intermediate Temperature Membranes

4

Jochen Kerres

4.1 Introduction

Among the most used materials as proton conductor in membrane fuel cells are sulfonated membranes such as the polymeric perfluorinated sulfonic acids (PFSA) of the Nafion® type [1]. Sulfonated membranes have the disadvantage that they require water as "vehicle" for proton transport through the membrane. Therefore, membranes based onto sulfonated polymers can only be used in fuel cells up to temperatures of 100 °C. However, it is desired that fuel cells can be operated at temperatures higher than 100 °C since an increase in temperature leads to the acceleration of electrode kinetics and therefore to an increase in fuel cell efficiency. Phosphoric acid is a proton conductor which has high proton conductivities over a large temperature range of up to more than 200 °C [2], but has the disadvantage being a liquid which makes its utilization as proton-conducting membrane in fuel cells impossible. To exploit the advantages of phosphoric acid for membrane fuel cells, the phosphoric acid molecules have to be immobilized in a solid matrix. Savinell et al. found that basic engineering polymers such as polybenzimidazoles [3, 4] (PBI) can be doped with phosphoric acid to an acid doping level (ADL) of more than four molecules of phosphoric acid (PA) per polymer repeat unit (PRU) and be used in this form as proton-conducting membrane in fuel cells in the temperature range >100 °C [5], where the phosphoric acid molecules in the membrane matrix build up a hydrogen bridge network which takes over the proton transport [6]. It should be noted that, in case of PBI blends with another acidic component, only the PBI component is taken into account in the ADL calculation and the unit is sometime written as PA/PRU(PBI).

A disadvantage of the H_3PO_4-doped polymer membranes is that they can bleed out a part of the phosphoric acid molecules when the operation temperature of the fuel cells falls below 100 °C and water produced by the fuel cell reaction condenses and dissolves H_3PO_4 [7]. The released H_3PO_4 can cause corrosion damage in the fuel cell system. A further disadvantage of a pure H_3PO_4-doped PBI is chemical degradation of the polymer [8]. As an alternative to polybenzimidazoles, other basic polymers such as pyridine moiety-containing aromatic main-chain polymers can be used. These types of basic polymers are reviewed in Chap. 5 of this book. In the past two decades, several strategies have been implemented to reduce the degradation and to improve the performance of the polymer in

---

J. Kerres (✉)
Institute of Chemical Process Engineering, University of Stuttgart, Boeblinger Str. 78, Stuttgart 70199, Germany

Focus Area: Chemical Resource Beneficiation, Faculty of Natural Science, North-West University, Potchefstroom 2520, South Africa
e-mail: jochen.kerres@icvt.uni-stuttgart.de

© Springer International Publishing Switzerland 2016
Q. Li et al. (eds.), *High Temperature Polymer Electrolyte Membrane Fuel Cells*,
DOI 10.1007/978-3-319-17082-4_4

fuel cell operation. Some of those strategies will shortly be reviewed here.

One possibility for improvement of chemical stability of the polybenzimidazole is the addition of nanoparticles to the polybenzimidazole. For example, OPBI (poly(4,4′-diphenylether-5,5-′-$32#bibenzimidazole)) has been blended with amine-modified silica nanoparticles (AMS) [9] or with nanodiamonds [10]. ABPBI (poly (2,5-benzimidazole)) has been modified with sulfonated silica nanoparticles [11]. Poly(2,2′-*m*-phenylene-5,5′-bibenzimidazole) (PBI Hozol®)-silica nanocomposites have been synthesized by a sol–gel reaction of tetraethoxysilane in the PBI matrix which was cross-linked to the PBI macromolecules by using (3-glycidoxypropyl)-methyldiethoxysilane [12]. Clay–PBI composites have been prepared by the addition of up to 20 wt % modified laponite clay to PBI solutions, followed by solvent evaporation [13]. It could be ascertained that the introduction of an inorganic phase to the PBI matrix led to mechanical reinforcement and improvement of thermal and chemical ex situ and in situ stabilities of the PBI membrane, and in some cases, as for example for ZrP-modified (ZrP = $(Zr(HPO_4)_2{\cdot}nH_2O)$) and H_3PO_4-doped PBI membranes, the proton conductivity of the inorganic PBI composite membranes was even higher than that of pure doped PBI [14].

Covalent cross-linking of PBI membranes is another possibility for improvement of their thermal, dimensional, and chemical stability. For example, the PBI can be cross-linked in the imidazole moiety with a low-molecular compound such as bisphenol A-diepoxide [15], divinyl sulfone [16], terephthaldehyde [17], α-dibromo-*p*-xylene [18], or dichloromethyl phosphonic acid [19]. Alternatively, the PBI membranes have also been cross-linked with macromolecular cross-linkers based onto halomethylated polymers, where the halomethyl groups alkylate the N–H group of the imidazole moiety. Halomethylated polymers, for example, chloromethylated PSU [20] or bromomethylated polyetherketone [21] have been applied for covalent cross-linking of high-T membranes. Covalently cross-linked high-T membranes are one of the topics of Chap. 9 of this book.

Another strategy for the improvement of the thermal, dimensional, mechanical, and electrochemical stability is the application of acid–base concepts to H_3PO_4-doped high-T basic polymers. The acid–base blend concept comprises blending of a basic polymer with an acidic polymer, where ionical acid–base cross-links are formed by proton transfer from the acidic group to the basic group (see Fig. 4.1).

The acid–base blend concept has been developed in the author's group about 16 years ago [22, 23] and was initially exploited for the preparation of low-temperature cation-exchange membranes, where the basic polymer was used as macromolecular basic cross-linker for the cation-conducting membranes (CEM) [24–27]. By ionical cross-linking of the cation-exchange polymer, the water uptake of the membrane could be reduced [25, 28], which led to improvement of the mechanical membrane stability. Moreover, it was observed that the ionical cross-linking of the CEM also led to an improvement of thermal stability (as could be proven by thermogravimetry (TGA) of the acid–base low-T CEM [27]) and resistance to radical attack (indicated by reduced weight loss of ionically cross-linked CEM after immersion in H_2O_2 solutions, compared to the pure acidic polymers [29]). By variation of the molar relation between basic and acidic polymers in the blend, the ion conductivity of the CEM could be varied in a broad range [27]. Hasiotis et al. [30] were the first to transform the acid–base blend concept to intermediate-T fuel cell membranes by mixing a molar excess of polybenzimidazole with sulfonated PSU, followed by doping with phosphoric acid and ex situ and in situ characterization of the formed ternary membrane blends. In these blends, the acidic polymer works as the macromolecular cross-linker in the blend membrane, and the phosphoric acid whose content in the membranes can be varied in a broad range (in the cited example the maximum ADL of the blend membranes was 16 [31]), provides H^+ conductivity of the membrane. In Fig. 4.2, the application of the acid–base blend concept to low-T and intermediate-T H^+-conducting membranes is presented schematically.

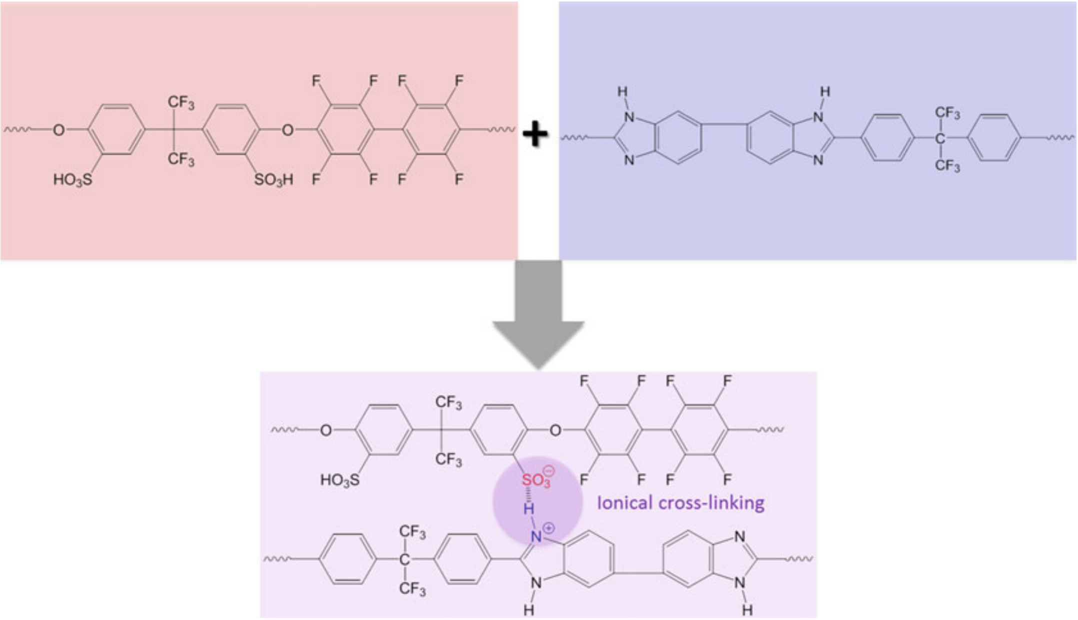

Fig. 4.1 Ionical acid–base cross-linking of an acidic and a basic polymer

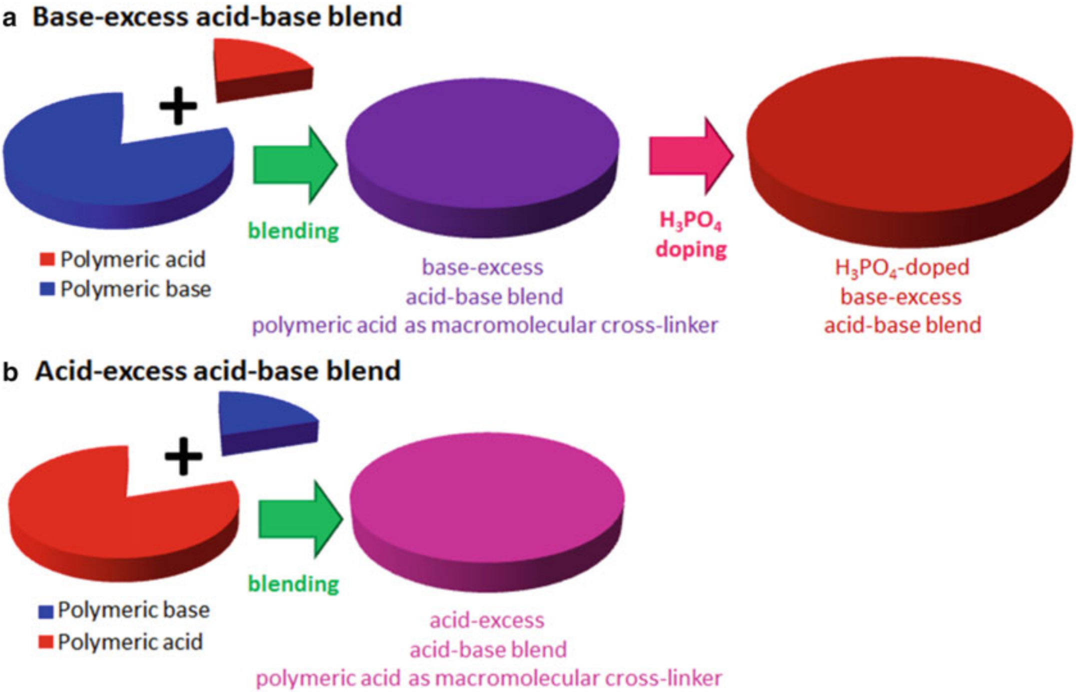

Fig. 4.2 The application of acid–base blend concept to intermediate-T (**a**) and low-T (**b**) H^+-conducting membranes

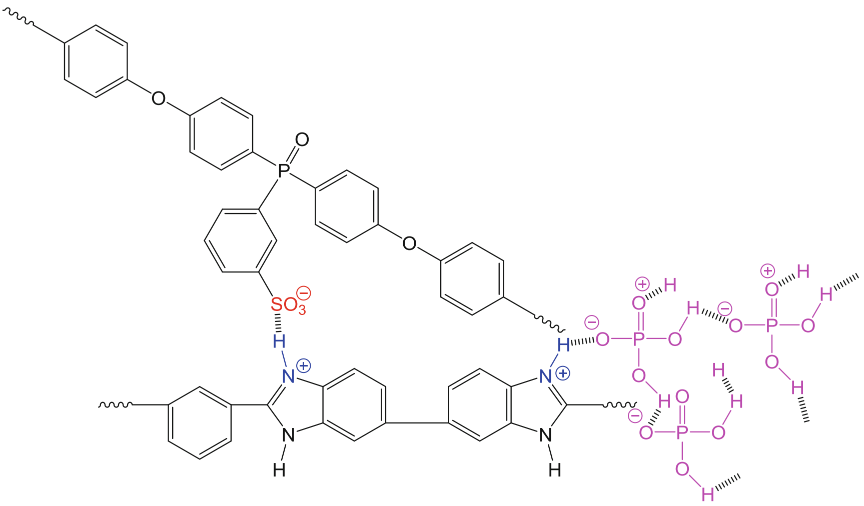

Fig. 4.3 Structure of an H_3PO_4-doped base-excess blend membrane based on PBI and sulfonated polymers

In Fig. 4.3, the structure of a PA-doped base-excess blend membrane based on PBI and sulfonated polymers is depicted schematically along with the hydrogen bridges between the H_3PO_4 molecules. In ongoing research, the author's group also started synthesis and characterization of H_3PO_4-doped base-excess acid–base blend membranes for the application in intermediate-T fuel cell systems. The research work done in the application of acid–base blend concepts to intermediate-T electrochemical applications will be reviewed in Sect. 4.2 of this contribution. This chapter will be concluded by a short comparative study covering covalently cross-linked, covalent-ionically cross-linked and ionically cross-linked intermediate-T polybenzimidazole blend membranes (Sect. 4.3).

4.2 State of the Art of the Application of Acid–Base Blend Concepts

The scope of the reviewed R&D work is limited to intermediate-T acid–base blend membranes prepared by mixing polybenzimidazoles and sulfonated or phosphonated acidic polymers. Other membrane types, where the acid–base concept was used to improve their relevant properties such as proton conductivity, and mechanical and chemical stability, are not discussed in this chapter, but are briefly mentioned below:

- Polybenzimidazoles with pendent acidic groups: sulfopropylated polybenzimidazole [31], sulfonated polybenzimidazole by the grafting of (4-bromomethyl)benzenesulfonate onto PBI [32], phosphonated fully aromatic polyethers containing pyridine building blocks [33], sulfonated aromatic polyethers containing pyridine units [34], sulfonated polybenzimidazoles from sulfonated dicarboxylic acid monomers [35–37].
- Polybenzimidazoles with grafted ionomer side chains: grafting-through and grafting-from polymerization of vinylphosphonic acid onto PBI [38–40].
- Poly(benzimidazole-block-sulfonated arylene ether sulfone)s [41].

In the following, those publications dealing with synthesis and characterization of intermediate-T blend membranes from PBI basic polymers and sulfonated or phosphonated polymers utilized as acidic macromolecular cross-linkers in the blends are discussed. In Fig. 4.4, those polybenzimidazoles along

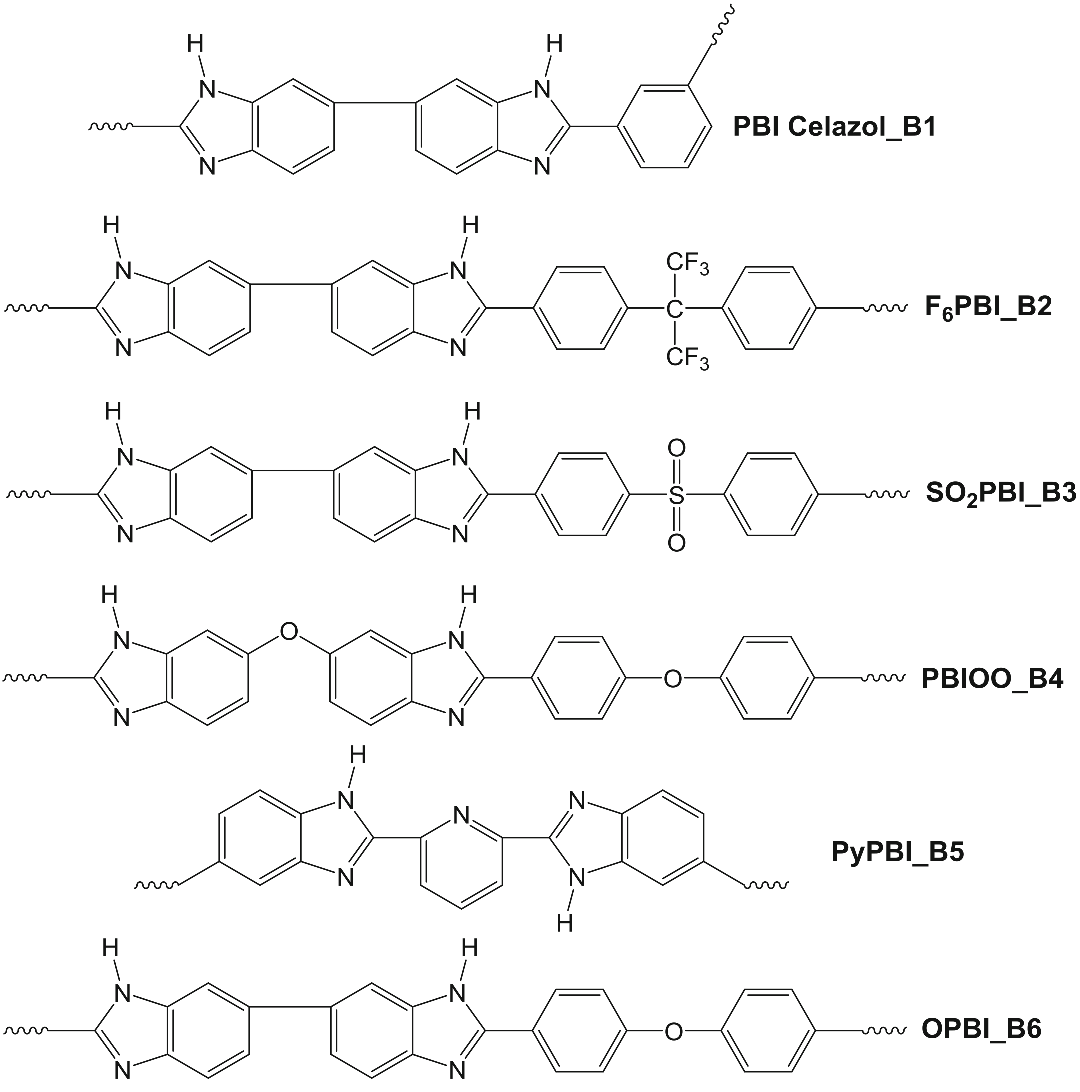

Fig. 4.4 Polybenzimidazoles used as basic blend components in acid–base blends which are reviewed in this chapter

with their abbreviations used as basic blend components in base-excess acid–base blends are depicted. In Fig. 4.5, all acidic polymers which were used as macromolecular ionical cross-linkers in the reviewed publications are listed.

As already mentioned, the acid–base blend concept was applied to intermediate-T fuel cell membranes by Hasiotis et al. [31, 42]. The blend membranes were composed of PBI Celazol® (poly(2,2′-*m*-phenylene-5,5′-bibenzimidazole, m-PBI, named as **B1**) and polysulfone Udel® sulfonated in the bisphenol A section (named **S1** in the following, see Fig. 4.5) [43]. Blend compositions (in wt%) from 100 **B1**/0 **S1** up to 50/50 were investigated. It was noted that the acid doping level decreased with decreasing PBI content which can be traced back to both the ionical cross-links by interactions of **S1** with **B1** and by decreasing **B1** proportion in the blend: for the 50/50 blend, a maximum ADL of 8.5 with respect to the PBI component was reached, while the pure **B1** maximal ADL was 16. The ionic conductivity of the blend membranes was measured in dependence of temperature, acid

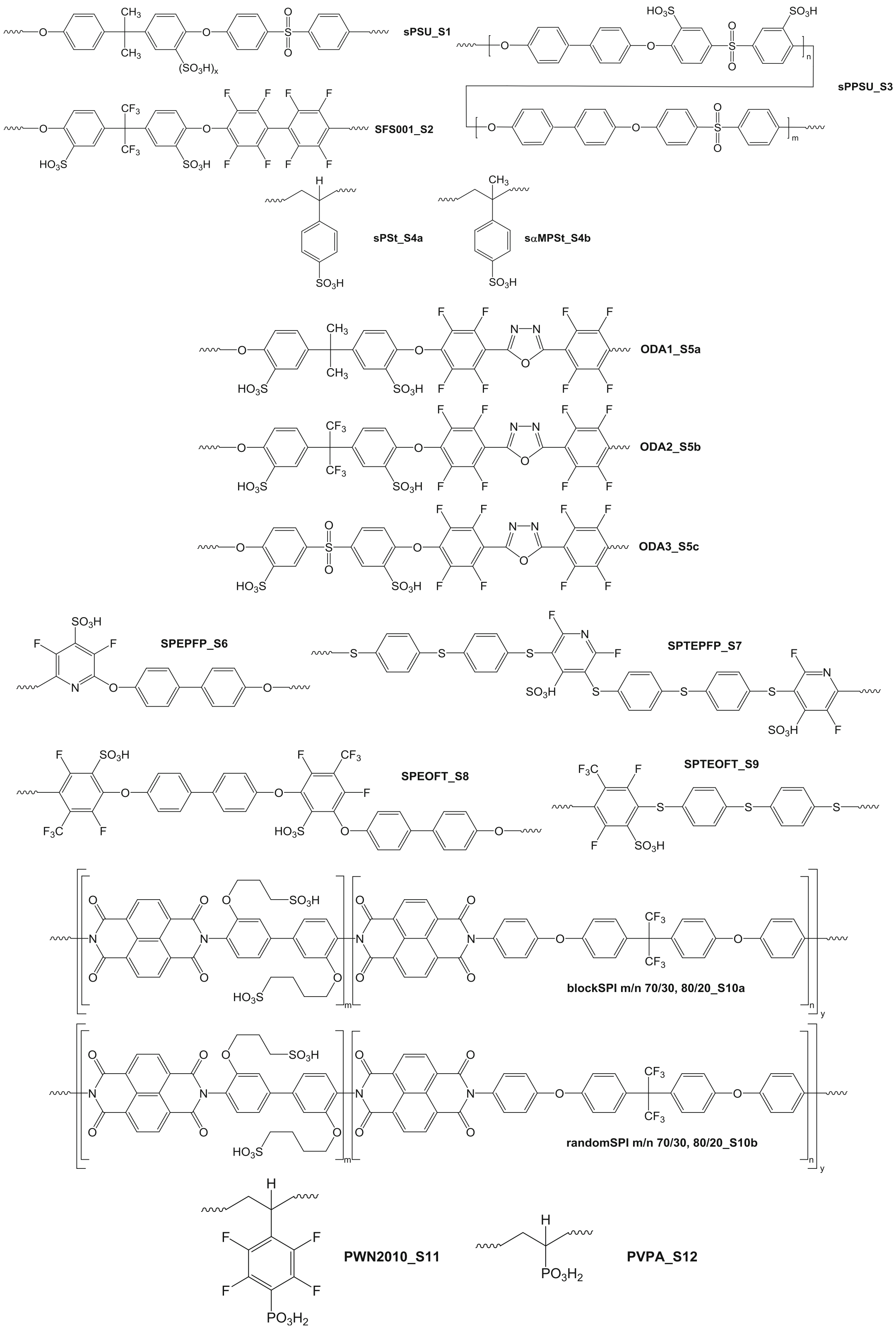

Fig. 4.5 Acidic polymers used as macromolecular ionical cross-linkers in acid–base-blend membranes mentioned in this review

doping level, sulfonation degree, relative humidity, and blend composition.

It was found that the doped blend membranes exhibited higher conductivities (in excess of 0.1 S cm^{-1}) than pure **B1** when applying equal doping conditions. The blend membranes showed strongly improved tensile strength, compared to pure **B1** which can be explained by the ionical cross-links within the membrane.

An H_2/O_2 fuel cell test of one of the blend membranes (75 % **B1**, 25 % **S1** with sulfonation degree of 36 %, ADL 4.6) indicated the principal suitability of this membrane type for intermediate-T fuel cells (0.45 mA cm^{-2} at 0.6 V). Since **S1** which is sulfonated in the bisphenol A portion in *ortho* position to the electron-donating ether bridge and in *meta* position to the also electron-donating isopropylidene bridge is therefore prone to splitting-off of the SO_3H groups in acidic environments in the T range around 200 °C [44, 45], which is within the operation temperature range of intermediate-T fuel cell systems, it would be advantageous to use such sulfonated polymers as ionical cross-linkers for PBI which show less sensitivity to hydrolytic/acidic (*ipso* reaction) and thermal splitting-off of its SO_3H groups.

Therefore, in a comparative study, different nonfluorinated and partially fluorinated sulfonated aromatic polymers were synthesized and characterized in terms of chemical and thermal stabilities. It was found that SO_3H groups introduced in the electron-deficient sections of the aromatic polymer main chains were much more stable against splitting-off than SO_3H groups pendent to electron-rich sections of the polymer backbones [29]. One of the most stable polymers of this series was a polymer prepared by polycondensation of decafluorobiphenyl and bisphenol (AF), followed by sulfonation with oleum (60 % SO_3), where the sulfonic acid groups were introduced into the bisphenol AF section of the polymer in *meta* position to the strongly electron-attracting perfluoroisopropylidene bridge. In [46], the synthesis of this polymer (named **S2**, Fig. 4.5) was optimized in terms of molecular weight (up to a stoichiometric imbalance decafluorobiphenyl:bisphenol AF of 0.995:1 non-cross-linked polymers could be obtained with $M_w = 204{,}500$ Da) and sulfonation degree (max. two SO_3H groups per repeat unit were obtained with oleum containing 50 % SO_3). It was noted that even oleum containing 50 % SO_3 did not lead to a degradation of **S2** in terms of molecular weight and sulfonation degree. Therefore, it was concluded that this polymer is a suitable candidate as acidic macromolecular cross-linker for PBI polymers. Consequently, base-excess blend membranes of **S2** have been prepared with **B1** (weight relation **B1**/**S2** 95/5, 90/10, 80/20, and 70/30). The blend membranes were characterized in terms of solubility by immersion in 60 °C hot DMAc, and by treatment with H_2O_2 (5 % H_2O_2, 60 °C), and Fenton's Reagent (3 % H_2O_2, 4 ppm Fe^{2+}, 68 °C [47]). The obtained results (only comparison between pure **B1** and 70/30 **B1**/**S2** is shown) are listed in Table 4.1.

In a further paper, the properties of H_3PO_4-doped pure **B1** and the 70 **B1**/30 **S2** were determined, including dependence of volume swelling, mechanical properties (stress–strain curves, tensile strength, elongation), and proton conductivity from ADL and temperature [48]. It could be ascertained that the blend membranes showed excellent mechanical strength and low swelling at high ADLs of 10–13 mol H_3PO_4 per PBI repeat unit. The stabilizing effect of the acid–base cross-links can be clearly seen from Table 4.1.

Table 4.1 Results of stability tests in different solutions for pure PBI **B1** and 70/30 **B1**/**S1** blend membrane

Membrane	60 °C DMAc	60 °C 5 % H_2O_2	Fenton's reaction
	Undissolved (wt%)	Undissolved (wt%)[a]	Undissolved (wt%)[b]
100 % **B1**	Dissolved after <1 h	20	61
70/30 **B1**/**S2**	90	10	84

[a] After 96 h of immersion

[b] After 120 h of immersion

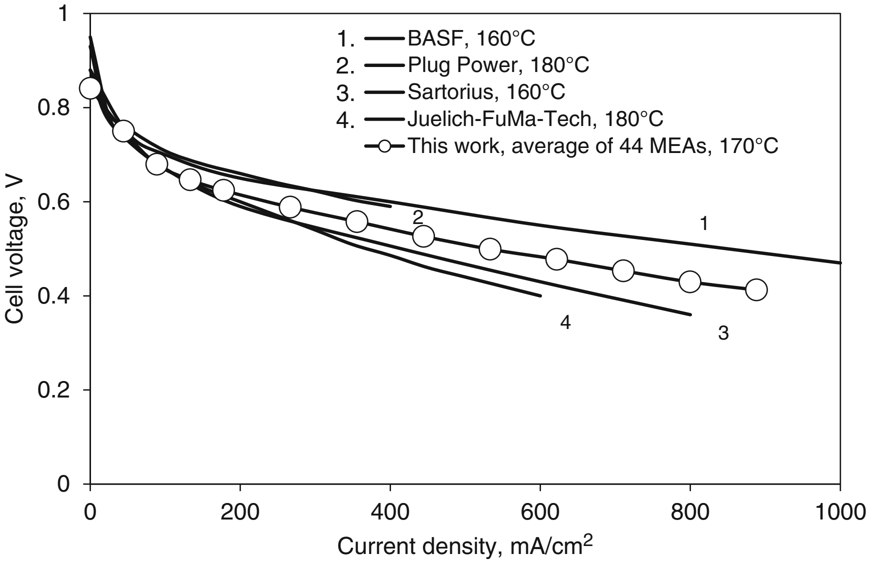

Fig. 4.6 Fuel cell performance of PBI cells (H_2/air), $T = 160–180$ °C (ambient pressure) [49]. The polarization curve was an average of 44 MEAs using **B1**/**S1** 70/30 (11 mol H_3PO_4 PBI repeat unit). Electrodes (256 cm^2): 48.6 % Pt/C catalysts, Pt loading of 0.6–0.7 mg cm^{-2}. Curves *1* by BASF [50] and Curve *2* by PlugPower [51] based on PPA (polyphosphoric acid) membranes, Curve *3* by Sartorius [52] based on PBI membrane cast from DMAc, Curve *4* by Juelich [53] cross-linked AB-PBI (FuMa-Tech). Reproduced with permission of Wiley-VCH

At an ADL of 11, H^+-conductivities of 0.12 S cm^{-1} (175 °C, 10 % relative humidity) were measured with the 70/30 blend membranes which showed the following mechanical properties: tensile strength of 6 MPa, elongation of 220 %, modulus of 50 MPa at 150 °C. From this membrane, MEAs with an active area of 256 cm^2 have been prepared, which have been tested in a 2 kW_{el} stack and showed good performance. In Fig. 4.6, the polarization curve of the 70/30 blend is shown at 170 °C operation temperature along with the polarization curves of other PBI-type membranes.

In a follow-up study, combinations of three different polybenzimidazoles with the partially sulfonated ionomer **S2** were investigated comparatively in terms of their stabilities to identify which **S2**/PBI combinations showed the best stabilities [49]. As polybenzimidazoles, **B1**, **B2,** and **B3** have been used in this study. All blend membranes contained 70 wt% of the polybenzimidazole and 30 wt% of **S2**. The blend membranes have been characterized in terms of oxidative stability by immersion in Fenton's Reagent for up to 120 h and subsequent determination of weight loss by gravimetry, molecular weight distribution by gel permeation chromatography (GPC) or size exclusion chromatography (SEC), and thermal stability by thermogravimetry. Some of the chemical stability characterization results of the blend membranes and of the pure PBIs are listed in Table 4.2.

From Table 4.2 it can be seen that, in terms of weight loss after FT, both the pure **B2** and the **B2S2** membranes show the best stabilities. The onset of SO_3H group splitting-off tempera tures ($T_{\mathrm{onset}}^{\mathrm{SO_3H}}$) of two of the blend membrane types (**B1S2** and **B2S2**) remains nearly constant which indicates that the structure of **B1** and **B2** is obviously chemically unchanged by Fenton's Test, while the decrease of $T_{\mathrm{onset}}^{\mathrm{SO_3H}}$ of **B3S2** and the increase of $T_{\mathrm{onset}}^{\mathrm{SO_3H}}$ of **B3** are inconsistent and need more detailed research. When comparing the values of the $T_{\mathrm{onset}}^{\mathrm{SO_3H}}$ of the different blend membranes with each other, the following series of $T_{\mathrm{onset}}^{\mathrm{SO_3H}}$ is detected: $T_{\mathrm{onset}}^{\mathrm{SO_3H}}$ (**B1**) > $T_{\mathrm{onset}}^{\mathrm{SO_3H}}$ (**B2**) > $T_{\mathrm{onset}}^{\mathrm{SO_3H}}$ (**B3**). This finding was explained by decreasing basicity of PBIs in this series,

Table 4.2 Characterization results of the blend membranes (and of pure PBIs, where applicable) before and after Fenton's Test (FT)

Membrane	Weight loss after 120 h FT	$T_{onset}^{SO_3H}$ (onset temperature of SO_2 signals)[a]	
		Before FT	After 120 h FT
B1	21.2	n.a.	n.a.
B1S2	13.2	434	438
B2	7.7	n.a.	n.a.
B2S2	2.04	417	416
B3	11	438[b]	466[b]
B3S2	7.9	403	380

[a] The determination of onset-temperature of SO_3H splitting-off by TGA-FTIR coupling is described in detail in [54]

[b] SO_2 signal originates from backbone degradation of SO_2PBI (**B3**)

since the ionical cross-links are stronger when the basicity of the respective PBI is higher. It can be summarized that in terms of chemical stability of PBIs, it is advantageous to choose polybenzimidazoles which consist of electron-deficient aromatic systems, as in the case of **B2** and **B3**. In terms of stability of the acid–base cross-links, one can see clearly that the $T_{onset}^{SO_3H}$ of all blend membranes are markedly above the fuel cell operation temperatures. GPC investigations of the pure PBIs and of their blend membranes before and after FT yielded the result that molecular weight degradation is clearly visible. However, the membranes still keep their mechanical integrity even after 120 h of FT which can be traced back to the ionical cross-links of the membranes which hold together the macromolecular chains of the blend components even after some degradation of the macromolecules has taken place.

Moreover, the blend membranes have been characterized in terms of acid doping, swelling, mechanical properties such as tensile strength, elongation and modulus, and proton conductivities. Two of the membranes were also tested in an H_2-air fuel cell. It was clearly indicated that volume swelling of the pure PBIs, **S2** and **S3** and their blend membranes at the same doping level was lower than that of **B1** and **B1S2**. This finding was explained by increasing free volume of the **B2** and **B3** membranes, compared to **B1**, due to the introduction of S, O, and F heteroatoms into the PBI, leading to an increase of van der Waals volume: when the membranes are doped with phosphoric acid (PA), the free volume is occupied by PA molecules before volume swelling takes place. In terms of mechanical properties, it was found that the blends showed clearly better properties due to the ionical cross-links. Since the blend membranes show much higher mechanical stabilities than pure PBIs, they could be doped to much higher degrees (doping level of pure PBIs between 7.1 and 8.3 mol H_3PO_4 (PA) and of PBI-**S2** blends between 10.9 and 13.3 mol PA per PRU(PBI)), which led of course to better proton conductivities of the blend membranes at the same temperature and relative humidity. At a PA doping level of 11, the **B2S2** membranes reached 0.135 S cm^{-1} at 10 % relative humidity (RH), while for the **B3S2** membranes conductivities of 0.145 S cm^{-1} were found under 10 % RH. The three blend membranes were operated in a fuel cell. The obtained polarization curves are shown in Fig. 4.7 [50], indicating good performance which, however, requires further improvement of the electrode design.

From the abovementioned results, it can be concluded that the combination of the partially fluorinated sulfonated ionomer **S2** with the partially fluorinated PBI **B2** is of advantage in terms of chemical stability and compatibility, which can be explained with chemical similarity, since both blend components consist of electron-deficient aromatic ring systems. Good PBI blend membrane stabilities can be achieved by good compatibility between the blend components, electron-deficiency of the aromatic ring systems, or both. To get hints of which is the

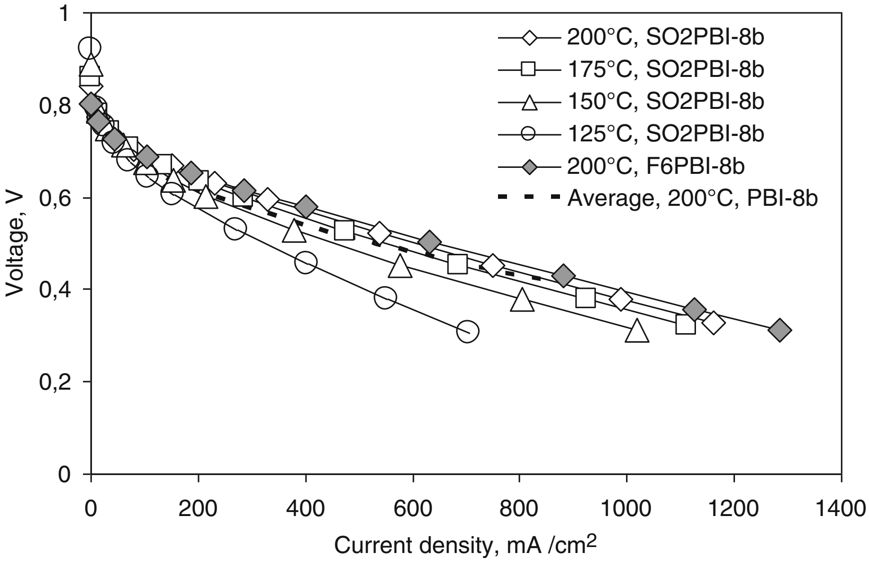

Fig. 4.7 Polarization curves of the **B2S2** (ADL 9.8 PA/PRU), **B3S2** (ADL 8.9 PA/PRU), and **B1S2** (ADL 11 PA/PRU) blend membranes [50]. Electrodes: 0.6 mg Pt cm^{-2} from 40 % Pt/C catalyst, binder: pure **B1**. Operation temperatures as indicated in the figure. Reproduced from [50] with permission of Elsevier

Table 4.3 FT and PA doping results of the PBI blend membranes [56]

Membrane	FT mass loss after 48 h (wt%)	FT mass loss after 120 h (wt%)	ADL[a]	PA doping degree[b]	PA swelling (x direction) (%)
B2S2	1.5	2	9.3	120	7
B2S3	4.4	22.5	23.4	300	14
B2 (Table 4.2 [50])	2.5	7.7	n.a.	n.a.	n.a.
B4S2	4	8.9	13.6	224	33
B4S3	1.6	7.6	17	280	20
B4 [56]	8.9	23.9	n.a.	n.a.	n.a.

[a] Mol PA/PRU(PBI)
[b] Calculated according to PA uptake (%) $= 100 \times m_{\mathrm{PA}}/m_{\mathrm{membrane\ dry}}$

main factor, a further study was performed, which included the preparation and characterization of different combinations of the electron-deficient partially fluorinated sulfonated ionomer **S2** or the more electron-rich nonfluorinated sulfonated ionomer **S3** (see Fig. 4.5) with the electron-deficient partially fluorinated PBI **B2** or the electron-rich nonfluorinated PBI PBIOO (**B4**) [55]. The following blend membranes were prepared, and their properties compared to each other: **B2S2**, **B2S3**, **B4S2**, and **B4S3**. In every case, the blend membranes contained 70 wt% of the PBI and 30 wt% of the sulfonated polymer. As in the aforementioned study, the membranes were subjected to FT for up to 120 h of Fenton's Reagent treatment time. Moreover, the membranes were PA-doped with 85 % PA for 30 min at 130 °C, and subsequently left in the PA solution for a further 30 min at room temperature. The FT and PA doping results are listed in Table 4.3. From the experimental results presented in Table 4.3, the following conclusions can be made:

- Like in the previous studies, the blend membranes show better FT stabilities than the pure PBIs because of the ionical cross-links.

- There is a clear trend that it is advantageous to combine chemically similar blend components with each other, since the **B2S2** and **B4S3** membranes indicate better FT stability than the electron-rich/electron-deficient blend mixtures.
- The **B4** blend membranes take up more PA under the same conditions than the **B2** blend membranes which can be traced back to the different stiffness and the different hydrophobicity of the PBI chains: the **B4** macromolecules are more flexible and more hydrophilic due to two O bridges in their repeat unit than the **B2** membranes featuring the more bulky and hydrophobic perfluoroisopropylidene unit.

The pure PBIs and PBI blend membranes have been investigated before and after FT in terms of molecular weight degradation using GPC. It was found that the molecular weight distribution (MWD) curves shift to somewhat lower molecular weight, but the MWD decrease was not very pronounced, which confirms the excellent radical stabilities of the blend membranes as already indicated by the weight losses of the membranes through FT. The PA-doped blend membranes were operated in an H_2/air fuel cell. The PA-doped **B4S3** membrane showed one of the best performances found for intermediate-T fuel cell membranes [49, 56, 57] without fuel cell gases pressurization, without humidification and without elaborated MEA preparation techniques, reaching a peak power density of 0.475 W cm^{-2} at 180 °C. The polarization curves of **B4S3** and **B2S2**, respectively, in the temperature range 120–180 °C are depicted along with the power density vs. current density curves at 180 °C in Fig. 4.8. Interestingly, the polarization curves of **B2S2** increase up to 130 °C and decrease at higher operation temperatures, while the **B4S3** exposes the expected improvement of polarization curves with temperature. The reason for this opposite behavior might be the observed mechanical properties of the two membranes: while the PA-doped **B4S3** has a gel-like structure with stronger bound PA, the PA-doped **B2S2** is more rigid due to the stiffer backbone of **B2**, which makes bleeding-out of PA from the **B2S2** membrane matrix easier than from the **B4S3** membrane matrix. The main reason for the markedly better polarization curves of **B4S3**, compared to **B2S2**, is the significantly higher ADL of the **B4S3** membrane (Table 4.3). GPC characterization of the **B2S2** membrane before and after fuel cell revealed that no molecular weight degradation took place during the fuel cell test.

In a further study, it was investigated if sulfonated low-cost ionomers can also be used as acidic cross-linkers for PBI polymers in order to reduce membrane costs. For this purpose, sulfonated polystyrene (**S4a**, Fig. 4.5) and poly (α-methylstyrene sulfonic acid), (**S4b**, Fig. 4.5) have been blended with commercial PBIOO (**B4**, Fuma-Tech) to 70 wt% PBIOO/30 wt% sulfonated polystyrene blend membranes. The membranes were characterized in terms of chemical stability by the immersion in Fenton's Reagent, thermal stability in terms of TGA-FTIR coupling and in terms of proton conductivity after PA doping [58]. Poly(α-methylstyrene sulfonic acid) was chosen for comparison with sulfonated polystyrene since it is known that the main radical attack target of polystyrene is the tertiary C–H bond [59] which is not present in poly(α-methylstyrene), leading to verified better radical stabilities of poly(α-methylstyrene), compared to poly(styrene) [60]. In Table 4.4, the results of thermal and FT stability of the blend membranes **B3**/**S4a** and **B3**/**S4b** are listed.

It is clearly seen from the characterization results that (1) the chemical stability of the polystyrene sulfonic acid blends is in the blend much higher than in the pure polymers due to acid–base cross-linking, (2) the radical stability of the blend membranes is higher than that of pure **B4** which is again due to the ionical cross-linking, and (3) the radical stability of the **S4b** blend membrane is much better compared to that of the **S4b** blend membrane. The better radical stability of the **B4S4b** blend can also be seen

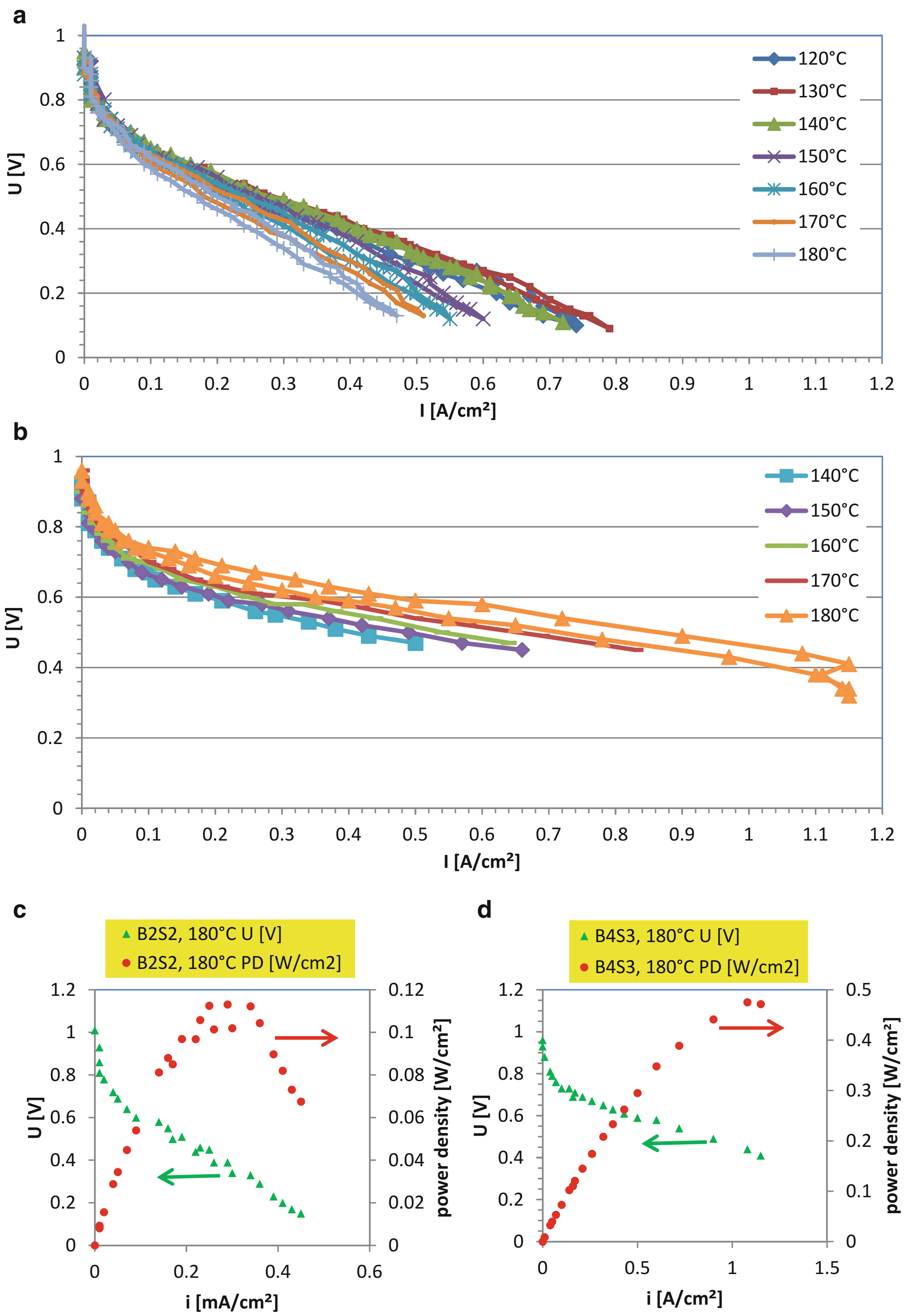

Fig. 4.8 Polarization curves of **B2S2** at temperatures between 120 and 180 °C (**a**), polarization curves of **B4S3** at temperatures between 120 and 180 °C (**b**) [56], selected polarization and power density curve of **B2S2** at 180 °C (**c**), and selected polarization and power density curve of **B4S3** at 180 °C (**d**). Figures (**a**) and (**b**) reproduced from [56] with permission of Elsevier

Table 4.4 Thermal stability (by TGA-FTIR coupling) and radical stability (by immersion of membranes for different times in Fenton's Reagent and subsequent weight loss and molecular weight loss determination) of **B4**/**S4a** and **B4**/**S4b**

Polymer/ membrane	$T_{\mathrm{onset}}^{\mathrm{SO_3H}}$ (°C)	Weight loss FT (%)
S4a	192	Dissolved after 24 h
S4b	213	Dissolved after 24 h
PBIOO_0 h FT (**B4**)	n.a.	
PBIOO_24 h FT	n.a.	13.5
PBIOO_120 h FT	n.a.	16
PBIOO_144 h FT	n.a.	16
B4S4a_0 h FT	379	
B4S4a_24 h FT	372	0
B4S4a_120 h FT	372	8
B4S4a_144 h FT	370	10
B4S4b_0 h FT	363	
B4S4b_24 h FT	365	0
B4S4b_120 h FT	356	3
B4S4b_144 h FT	357	3.5

very clearly in SEM micrographs of both membranes: while the surface of the **B4S4b** blend membranes only shows a few 1–4 μm-sized small craters due to the OH radical attack, the surface of the **B4S4a** blend membranes is highly porous, indicating strong radical attack [59]. PA doping experiments of the membranes revealed a faster PA uptake of the **B4S4b** membranes, compared to those of the **B4S4a** membranes, which can most probably be traced back to higher free volume of the **S4b** blends because of their bulky CH_3 groups. Moreover, it was found that the proton conductivities of the **B4S4b** membranes were higher (42 mS cm^{-1}) at the same ADL (18.2) (300 wt%) and temperature (120 °C) than those of the **B4S4a** membranes (30 mS cm^{-1}) which might also be a consequence of higher free volume of the **B4S4b** blends. Summarizing the results of this study, it was shown that low-cost ionomers can also be used as acidic cross-linkers for PBI-type membranes if the radical stability of the low-cost ionomers is sufficiently high due to the absence of oxidation-sensitive chemical bonds.

Since it could be shown that the partially fluorinated sulfonated arylene ionomer **S2** showed excellent oxidation stabilities as blend partner of the partially fluorinated **B2** (Table 4.3 [50, 56]), further partially fluorinated and sulfonated arylene ionomers based on the polycondensation of 2,5-bis(perfluorophenyl)-1,3,4-oxadiazole [61] with the three bisphenols bisphenol A, bisphenol AF, and bisphenol S, followed by sulfonation, have been synthesized [62]. The structure of the three sulfonated poly (perfluorooxadiazole) (sODA) ionomers is shown in Fig. 4.5 (sODA from bisphenol A: **S5a**; sODA from bisphenol AF: **S5b**; sODA from bisphenol S: **S5c**). It was noted that some molecular weight degradation of the sODA polymers takes place during sulfonation which might be due to the harsh reaction conditions of sulfonation since oleum was used as sulfonation agent. The sODA polymers were blended with the fluorinated **B2** and the nonfluorinated **B3** (70 wt% PBI, 30 wt% sODA), and the properties of the blend membranes were determined. Due to the fact that only the blend membranes containing **B2** showed good mechanical stabilities (the **B3**/sODA blends were brittle), the characterization was continued only with the **B2** blend membranes. The blend membranes were characterized in terms of thermal stability (TGA), oxidation stability (weight loss after FT), and conductivity after doping with PA. The characterization results are gathered in Table 4.5.

The characterization results suggested good suitability of this membrane type for intermediate T fuel cells. However, all fuel cell tests of the membranes failed because the membranes showed holes after relatively short fuel cell operation times. This finding can most probably be traced back to the too low-molecular weight of the sODAs after sulfonation (**S5a**: $M_w = 17{,}000$ Da; **S5b**: $M_w = 17{,}000$ Da; **S5c**: $M_w = 18{,}600$ Da) which leads to insufficient mechanical stabilities—the membranes were very soft after PA doping. Therefore, R&D work with these membranes was discontinued.

The search for further chemically highly stable partially fluorinated arylene ionomers as blend partners for polybenzimidazoles was

Table 4.5 Characterization results of **B2**/sODA blend membranes [63]

Membrane	$T_{\text{onset}}^{\text{SO}_3\text{H}}$ (sODA) (°C)	$T_{\text{onset}}^{\text{SO}_3\text{H}}$ (blend membrane) (°C)	Weight loss FT after 96 h (%)	Conductivity[a] (150 °C, 20 % RH) (S cm^{-1})
B2S5a	374	431	8.5	35
B2S5b	348	414	7	88
B2S5c	319	452	7	49

[a] PA doping degree: 300 wt%, ADL: 23.4

however continued. Due to the fact that high chemical and thermal stabilities and high proton conductivities can be expected from aromatic ionomers with pendent SO_3H groups in an electron-deficient aromatic environment, novel arylene ionomers have been prepared starting from the perfluorinated building blocks octafluorotoluene (OFT) and pentafluoropyridine (PFP). The SO_3H groups were introduced in both monomers following a nucleophilic route initially developed by other research groups [63–66]: first SH groups were introduced into pentafluoropyridine and octafluorotoluene by nucleophilic aromatic substitution with F, followed by oxidation of the SH groups with H_2O_2/HCOOH to SO_3H groups. The formed sulfonic acid monomers (2,3,5,6-tetrafluoro-4-(trifluoromethyl)benzenesulfonic acid (TFTF-BSA) and 2,3,5,6-tetrafluoro-pyridine-4-sulfonic acid (TFPSA), respectively), were then polycondensated with 4,4′-diphenol and 4,4-′-thiodibenzenethiol, respectively [67]. The structure of the resulting polymers **S6**, **S7**, **S8,** and **S9** is schematically depicted in Fig. 4.5. Interestingly, the structure of the polymers **S6**, **S8,** and **S9** is angled (revealed by ^{19}F NMR) which can be traced back to similar nucleophilic displacement reactivities of the different F atoms in the two monomers during polycondensation. The ionomers were then blended with the three PBIs: **B1**, **B2**, and **B3** in different proportions of the blend components. In Table 4.6, some properties of 70 % PBI/ 30 % sulfonated polymer blend membranes from **B1**, **B2,** and **B4** with **S6**, **S7**, **S8**, and **S9** are listed.

It can be clearly seen from Table 4.5 that the two polymers containing the sulfonated pyridine units (**S6** and **S7**) show bad radical stabilities in their blend membranes with **B1** which is indicated by the strong weight losses after 144 h of FT. Moreover, SEM micrographs of these membranes after FT showed highly porous surfaces, indicating strong membrane degradation by the radical attack [68, 69]—obviously the perfluoropyridine building blocks of **S6** and **S7** are prone to the radical attack degradation despite the electron-deficiency of their aromatic systems.

Therefore, the pyridine-containing sulfonated polymers were not used as acidic cross-linkers for blends with the other PBIs. On the contrary, the blends of **S8** and **S9** with the PBIs expose excellent radical stabilities indicated by very small weight losses after 144 h of FT (Table 4.5). Therefore, only blend membranes from **B1**, **B2,** and **B4** with **S8** and **S9** have been further investigated in terms of suitability for intermediate-T fuel cells [69]. The best fuel cell performance among all tested membranes was reached with a **B2S8** membrane (20 wt% **S8**) comprising a peak power density of 400 mW cm^{-2} at 1 A cm^{-2} (conditions: $T = 120$ °C, doping degree 400 wt% (ADL: 27.3), GDEs with Pt loading 3 mg Pt cm^{-2} which were simply pressed onto the membrane). It can be concluded that the PBI blend membranes containing **S8** and **S9** acidic cross-linkers offer good perspectives for use as membranes in intermediate-T fuel cells due to their excellent radical stabilities.

Apart from the work done under participation of the author of this study reported above, only a few papers have been published dealing with the synthesis and characterization of acid–base blend membranes. One of these publications is an article of Iizuka et al. who described the synthesis of novel sulfonated random or block co-polyimides (blockSPI, **S10a**, randomSPI, **S10b**, Fig. 4.5) [69] and their use as acidic blend components

Table 4.6 Some properties of 70 % PBI/30 % sulfonated polymer blend membranes from **B1**, **B2**, or **B4** with **S6**, **S7**, **S8**, and **S9** [68]

Membrane	M_n (PDI) (sulf. polymers) (Da) (–)	$T_{onset}^{SO_3H}$ (sulf. polymer) (°C)	$T_{onset}^{SO_3H}$ (blend membrane) (°C)	FT weight decrease after 144 h (%)
B1S6	5900 (1.74)	378	419	39
B1S7	12,500 (2.39)	328	359	27
B1S8	10,100 (2.89)	375	426	8
B1S9	15,000 (1.33)	329	442	9
B2S8	See above	See above	440	4.1
B2S9	See above	See above	425	2.9
B4S8	See above	See above	441	4.5
B4S9	See above	See above	397	1.8

of PBI blend membranes, where the PBI component OPBI (**B6**, Fig. 4.4) was the minor component with only 10 wt% share in the blend [70]. PA doping was performed by immersion of the membranes in 85 % PA for appropriate times. The motivation for preparation of this membrane type was that these membranes should have different proton transport pathways: in the temperature range between 0 and 100 °C, the proton conduction should be provided by the SO_3H groups and water, and at <0 and >100 °C via the PA H-bridge network. Indeed, the membranes possessed high proton conductivities between 0 and 100 °C (via the SO_3H/H_2O pathway, e.g., 0.37 S cm^{-1} at 90 °C and 98 % RH) and higher proton conductivities than Nafion above 100 and below 0 °C (via the PA pathway). It was thereby indicated that the block-type SPI/OPBI blends exhibit higher proton conductivities than the random-type SPI/OPBI blends at same IEC, PA doping degree, T and RH. The higher proton conductivity of block-co-ionomers, compared to random polymers of the same IEC, can be traced back to their nanophase-separated biscontinuous structure comprising proton-conducting channels of high SO_3H group density which facilitates proton conduction [71].

Apart from sulfonated polymers, it could recently be shown that phosphonated polymers can also be used advantageously as macromolecular ionical cross-linkers for PBI blend membranes: poly(tetrafluorostyrene-4-phosphonic acid) (PWN2010, **S11**, Fig. 4.5) was synthesized via nucleophilic aromatic substitution of poly(pentafluorostyrene) [72]. The phosphonated polymer was then mixed with PBIOO (**B4**, Fig. 4.4) in a molar relation imidazole/PO_3H_2 groups = 3/7 [73]. The so-formed blend membranes were characterized in terms of oxidation stability in Fenton's Reagent. It was found that obviously the **B4** blend component had worse chemical stability than the **S11**: while pure **S11** only lost 2 % weight after 96 h of FT (GPC analysis of the pure **S11** revealed only slight molecular weight degradation of low-molecular constituents of the **S11**), both pure **B4** and the **S11B4** membranes showed weight losses of 17 % after 96 h FT. However, it could be seen from SEM inspection of the pure **B4** and **S11B4** membrane surfaces that both membranes maintained their integrity and mechanical stability even after 96 h FT—they only showed some craters with diameters of roughly 10 µm in their surfaces originating from OH radical attack. While pure **S11** showed one of the highest dry proton conductivities measured for phosphonated polymers [74], the **S11B4** blend membranes had to be doped with phosphoric acid (PA) to increase their proton conductivity. A blend membrane doped with 270 wt% PA was operated in an air/H_2 fuel cell from 80 to 150 °C, showing good and increasing performance at an increase of operation temperature (Fig. 4.9).

Ongoing research on the **S11** acid–base ionomer membranes includes the blending of **S11** with **B2** which leads to blend membranes showing excellent oxidation stabilities even after immersion in FT for up to 144 h (see Sect. 4.3).

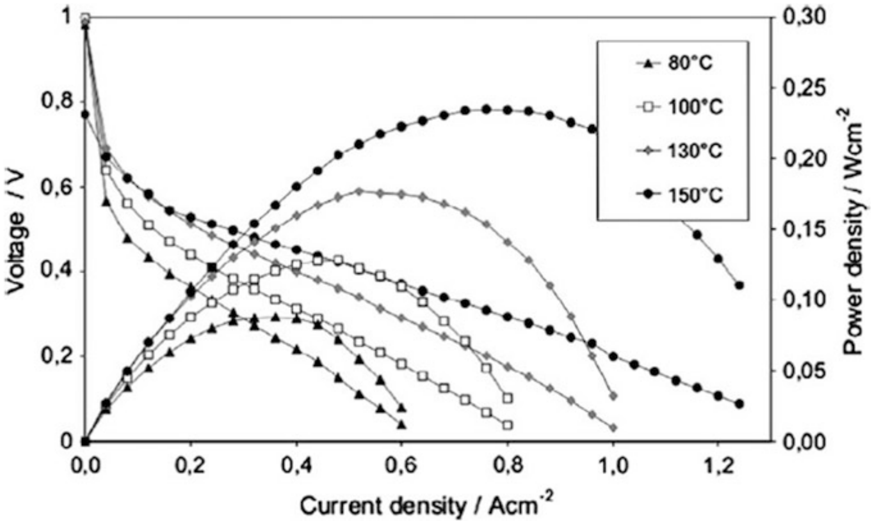

Fig. 4.9 Fuel cell test of an **S11B4** blend membrane, PA doping degree 270 wt% [74]. Reproduced with permission of Elsevier

In [74], completely phosphoric acid-free intermediate-T membranes and MEAs from 1/1 (mole imidazole/mole PO_3H_2) blend membranes of the PBI **B5** (Fig. 4.4) and the phosphonated polymer polyvinyl phosphonic acid (PVPA) **S12** (Fig. 4.5) were presented and compared to PA-doped membranes and MEAs. In the MEAs, a Pt electrocatalyst was deposited onto multiwalled carbon nanotubes (MWNT) which have previously been coated with **B5**. This technique has previously been used for the preparation of electrocatalysts for anion-exchange membrane fuel cells [75]. In the final step, the MWNTs were coated with a layer of **S12**. It turned out that these membranes and MEAs possessed much higher durabilities than membranes and MEAs which have been doped with PA, therefore opening leeway for long-lasting intermediate-T fuel cell membranes without the PA leaching problems which are always present in PA-doped intermediate-T membranes and MEAs [76].

4.3 Short Comparative Study of the Stability and Properties of PBI-Type Membranes

In this section, the properties of PBI-excess acid–base blend membranes will be compared to those of other PBI membrane types to consider the question of whether one of the investigated membrane types, if any, shows more advantageous properties than the others. The motivation for this short study was the difficulty of comparing the membrane characterization results from different literature sources since the individual characterization methods applied in these references are—in part—varying strongly. The ionically cross-linked PBI blend membranes reviewed in this chapter will be compared to the type of covalently cross-linked PBI blend membranes which has been mentioned in the introduction (blends of PBI with halomethylated polymers whose CH_2Hal groups partially react with the N–H groups of the imidazole moiety of the PBIs [21, 22]). In the third membrane type investigated in this short study, the concepts “ionically cross-linked blend” and “covalently cross-linked blend” have been combined by the preparation of covalent-ionically cross-linked blend membranes via mixing the PBI with both the halomethylated and the cation group-containing polymer.

The following blend components have been varied at the different membranes under investigation: the type of PBI (**B2** and **B4**, Fig. 4.4), the type of acidic macromolecular ionical cross-linker (sulfonated and phosphonated ionomer, **S2** and **S11**, respectively, Fig. 4.5), and the type of macromolecular covalent bromomethylated

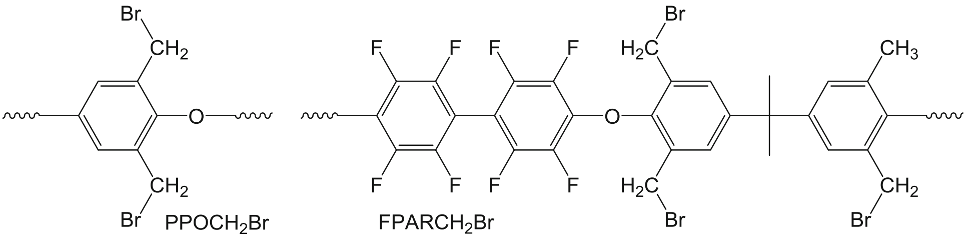

Fig. 4.10 The two investigated bromomethylated polymers

Table 4.7 Investigated blend membrane types

Membrane (No.)	PBI (wt%)	Acidic polymer (wt%)	Polymer-CH_2Br (wt%)	Type cross-linking
F_6PBI (**B2**)	**B2**: 100	–	–	None
1921C	**B4** (PBIOO): 80	–	$PPOCH_2Br$: 20 %	Covalently
1925C	**B2**: 80	–	$FPARCH_2Br$: 20 %	Covalently
1927A	**B2**: 80	**S2**: 20 %	–	Ionically
1938	**B2**: 80	–	$PPOCH_2Br$: 20 %	Covalently
1940	**B2**: 80	**S11**: 20 %	–	Ionically
1943	**B2**: 80	**S2**: 10 %	$FPARCH_2Br$: 10 %	Covalent-ionically

cross-linker (nonfluorinated $PPOCH_2Br$ and partially fluorinated $FPARCH_2Br$, respectively, Fig. 4.10).

The preparation (Fig. 4.1) and structure (Fig. 4.3) of an H_3PO_4-doped ionically cross-linked acid–base blend membrane (membranes 1927A and 1940 in Table 4.7) was already depicted schematically in the introduction. Figure 4.11 presents the preparation and the structure of a covalently cross-linked blend membrane (membranes 1921C, 1925C, and 1938), and Fig. 4.12 the preparation and structure of a covalent-ionically cross-linked blend membrane (membrane 1943).

The following properties of the membranes relevant for their potential application in fuel cells have been determined and compared among the different membranes involved in this study, including the benchmark membrane **B2**:

- Thermal stability via TGA
- Cross-linking degree/insolubles fraction by immersion in 90 °C hot DMAc
- Chemical stability via Fenton's Test (FT)
- Proton conductivity of H_3PO_4-doped membranes

Selected results of membrane characterization will be presented in the subsection below.

4.3.1 Thermal Stability of the Blend Membranes

The thermal stability of all membranes was determined via thermogravimetry under a 65–70 % O_2 atmosphere with a heating rate of 20 K/min [54]. Firstly, it was investigated whether the type of cross-linking influences the thermal stability of the membranes. Therefore, in Fig. 4.13, the TGA traces of the membranes 1925C (covalently cross-linked), 1927A (ionically cross-linked), and 1943 (covalent-ionically cross-linked) are presented together with **B2**.

The TGA traces suggest that the thermal stability of all membranes is similarly excellent up to temperatures of 300 °C which is far above the highest temperature applied in intermediate-T fuel cells (220 °C [77]). Only above 300 °C the influence of the thermally more instable polymer backbones of the other blend components apart from **B2** is apparent.

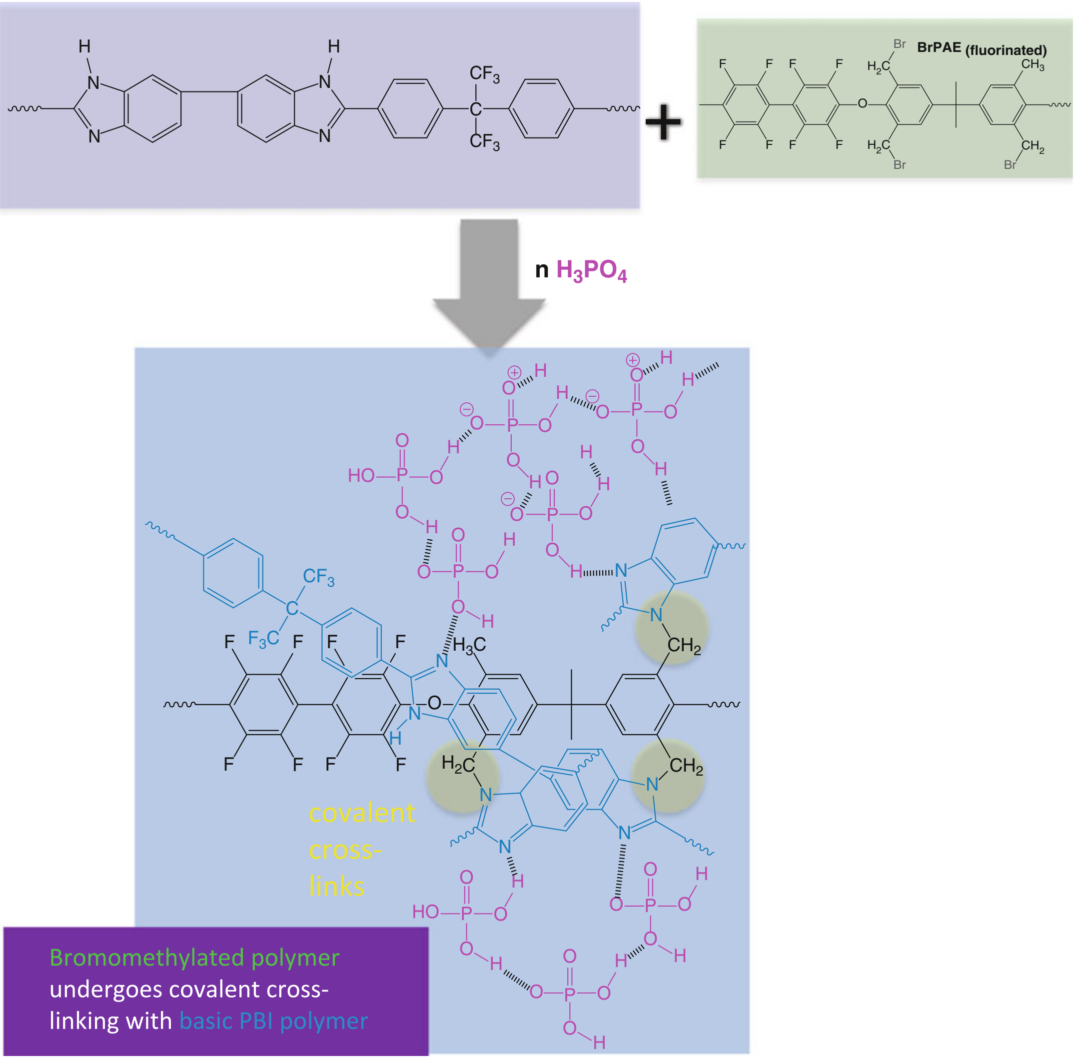

Fig. 4.11 Preparation and structure of covalently cross-linked intermediate-T blend membranes

Secondly, the possible influence of type of cation-exchange group of the acidic cross-linker was inspected. As functional groups for acid–base cross-linking, the strongly acidic sulfonic acid group or the medium-acidic phosphonic acid group are available. As cation-exchange polymers, the highly stable ionomers **S2** [46] and **S11** [73] have been selected. In Fig. 4.14, the TGA traces of the ionically cross-linked membranes 1927A (sulfonated ionical cross-linker **S2**, Fig. 4.5), and 1940 (phosphonated ionical cross-linker **S11**, Fig. 4.5) are depicted along with **B2**. Again, all TGAs indicate excellent and similar thermal stabilities of all membranes up to 300 °C. Therefore, it can be concluded that both sulfonated and phosphonated polymers can be selected as acidic cross-linkers for polybenzimidazole membranes.

Furthermore, covalently cross-linked membranes from **B2** and the two different covalent macromolecular cross-linkers $PPOCH_2Br$ and $FPARCH_2Br$ (Fig. 4.10) have been compared to each other and to **B2** in terms of TGA.

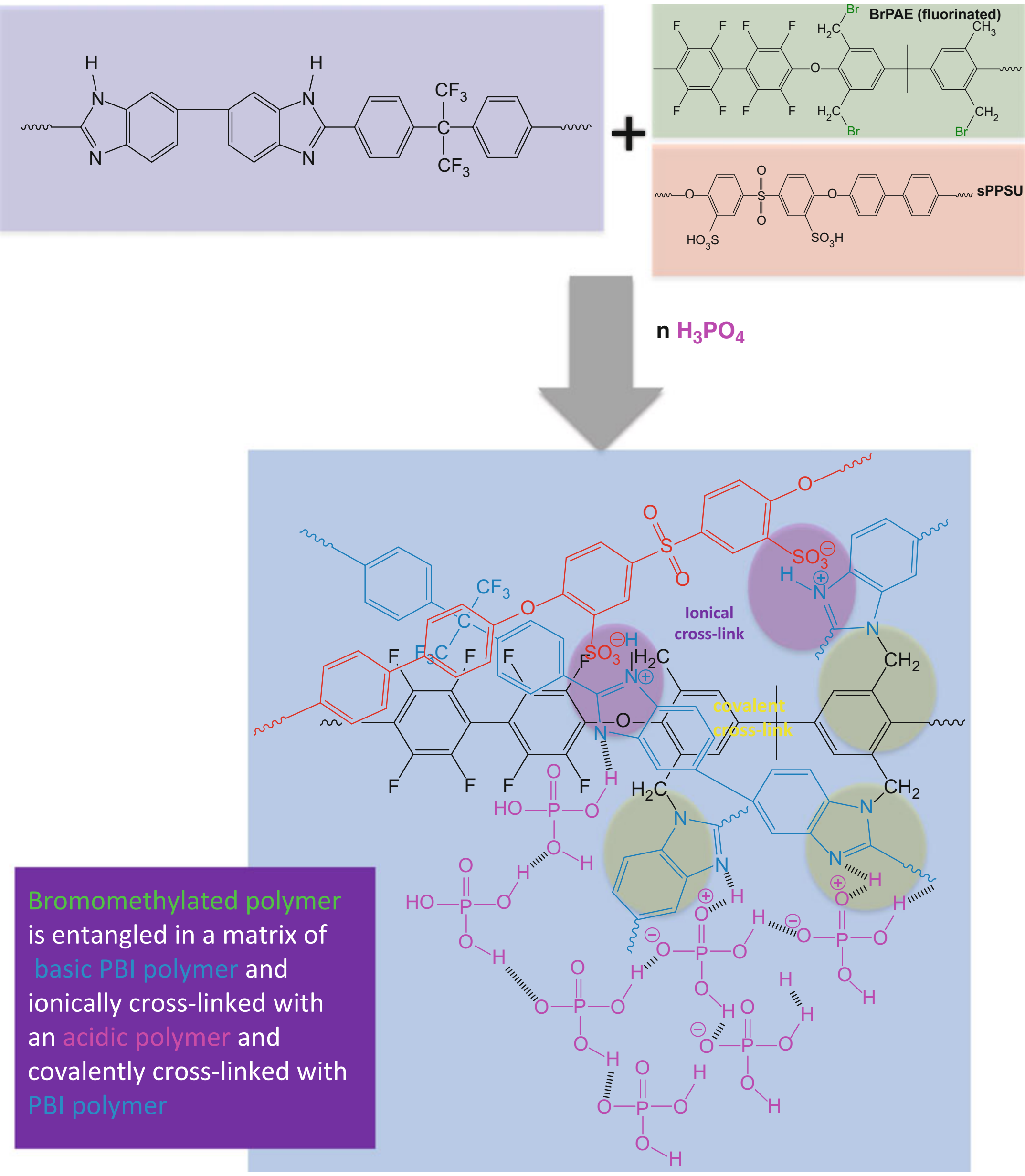

Bromomethylated polymer is entangled in a matrix of basic PBI polymer and ionically cross-linked with an acidic polymer and covalently cross-linked with PBI polymer

Fig. 4.12 Preparation and structure of covalent-ionically cross-linked intermediate-T blend membranes

Since PPOCH$_2$Br is a nonfluorinated, electron-rich polymer and FPARCH$_2$Br a partially fluorinated arylene polymer, one could conclude that the partially fluorinated arylene polymer introduces better thermal stabilities into the blend membrane (Fig. 4.15).

However, contrary to the expectation, both covalently cross-linked blend membranes possess nearly identical thermal stabilities in the whole TGA range, highlighting the dominant influence of the main blend component **B2** on the thermal membrane properties.

Moreover, a thermal stability comparison has been made between the covalently cross-linked (cross-linker: PPOCH$_2$Br) membranes 1921C (**B4**-containing) and 1938A (**B2**-containing).

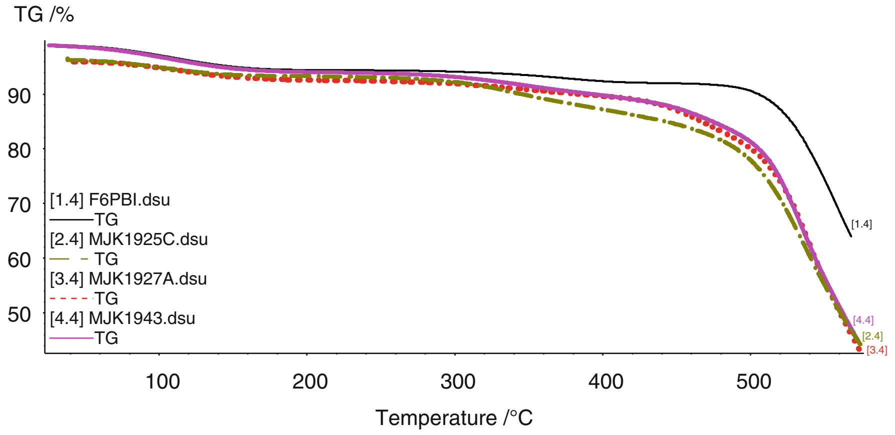

Fig. 4.13 TGA traces of membranes **B2**, 1925C, 1927A, and 1943

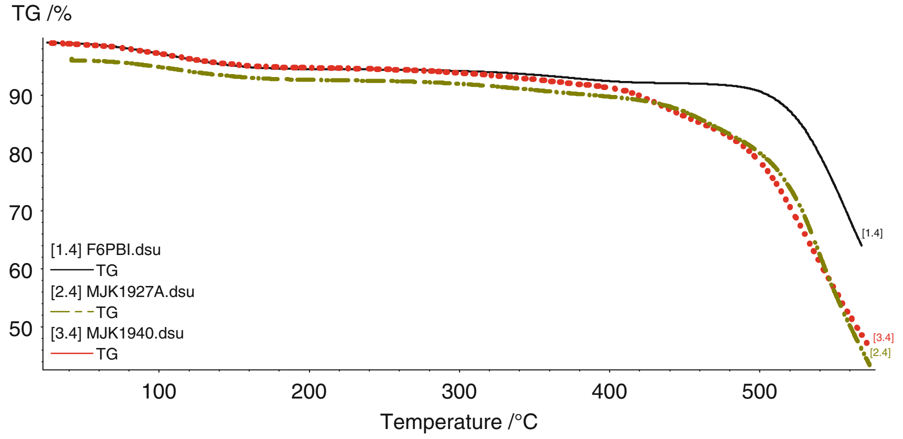

Fig. 4.14 TGA comparison of **B2**, 1927A (sulfonated ionical cross-linker **S2**, Fig. 4.5), and 1940 (phosphonated ionical cross-linker **S11**, Fig. 4.5)

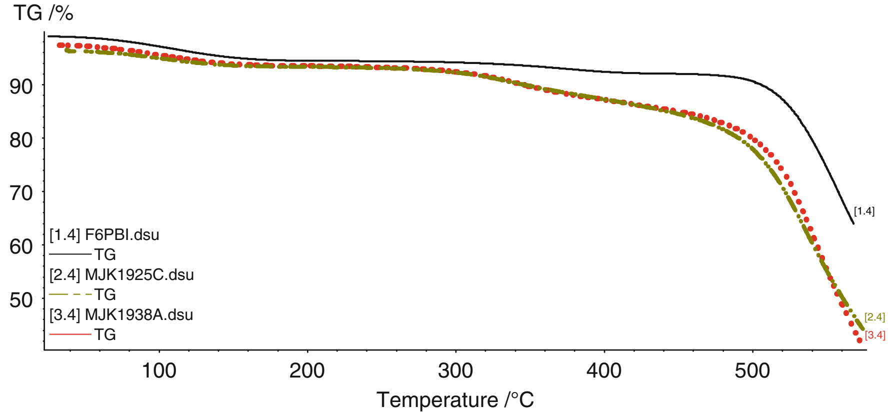

Fig. 4.15 TGA comparison of **B2** with the blend membranes 1938A (PPOCH_2Br as cross-linker) and 1925C (FPARCH_2Br as cross-linker)

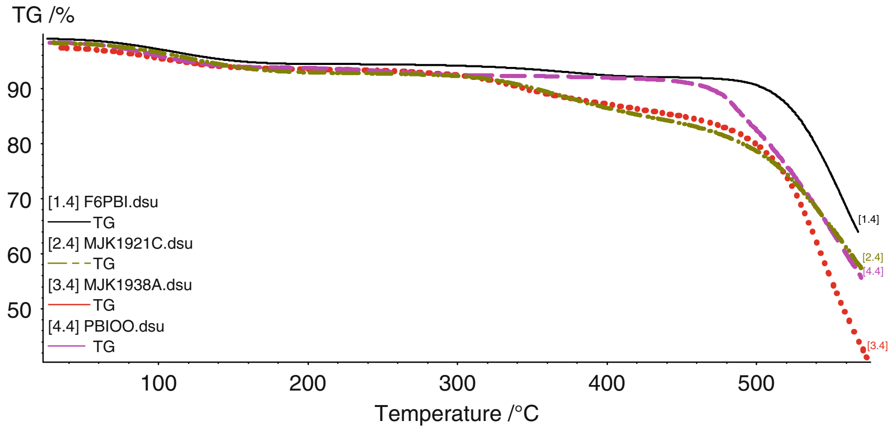

Fig. 4.16 TGA comparison of 1921C (**B4**-containing) and 1938A (**B2**-containing) and pure **B2** and **B4**

The TGA traces of pure **B2** and **B4** have also been included in Fig. 4.16.

From Fig. 4.16 can be read that both covalently cross-linked blend membranes expose nearly similar thermal stabilities, while the thermal stability of pure partially fluorinated **B2** is slightly better than that of the pure fluorine-free **B4** only above 450 °C which is however not relevant for the intended intermediate-T fuel cell application of these membranes. Therefore, covalent cross-linking can be regarded as a good method to improve thermal (and chemical, see below) stabilities of PBI-type membranes.

It can be concluded from the obtained TGA results that all of the investigated PBI blend membranes show, regardless of cross-linking and cross-linker type, comparable thermal stabilities. At higher contents of the non-PBI blend components, the property differences between the different intermediate-T blend membrane types might be more strongly pronounced.

4.3.2 Cross-linking Degree/Insoluble Fraction by Immersion in 90 °C Hot DMAc

The insoluble fraction after the extraction of the membranes in 90 °C hot DMAc is a measure of the extent of cross-linking of the membrane matrix. The extraction results (the extraction method is described in [78]) are presented in Fig. 4.17. As expected, the pure PBIs completely dissolve in hot DMAc. Interestingly, the ionically cross-linked membranes remain partially undissolved which is an indication for relatively strong acid–base and hydrogen bridge interactions. The phosphonated blend component obviously forms even stronger interactions with the PBI than the sulfonated blend component (insolubles at membrane 1927A = 61.8 %, insolubles at membrane 1940 = 81.7 %) which can most probably be traced back to the two acidic OH groups present per PO_3H_2 group in the phosphonated ionomer **S11** that are available for ionical cross-linking. The three covalently cross-linked membranes (1921C, 1925C, 1938A) and the covalent-ionically cross-linked membrane comprise large insoluble fractions of clearly above 90 %, indicating complete formation of cross-linked network within the membranes. The cross-linked network is an important prerequisite for stability of PBI-type membranes to be applied to PA-doped intermediate-T fuel cells since it was reported that pure PBIs can dissolve during PA doping as it was observed with pure **B4** [59].

The membranes gathered in Table 4.7 were immersed in Fenton's Reagent according to the reviewed literature (e.g., [47]) for 144 h, and after this time the weight loss was determined. The amount of weight loss of membranes is represented in Fig. 4.18.

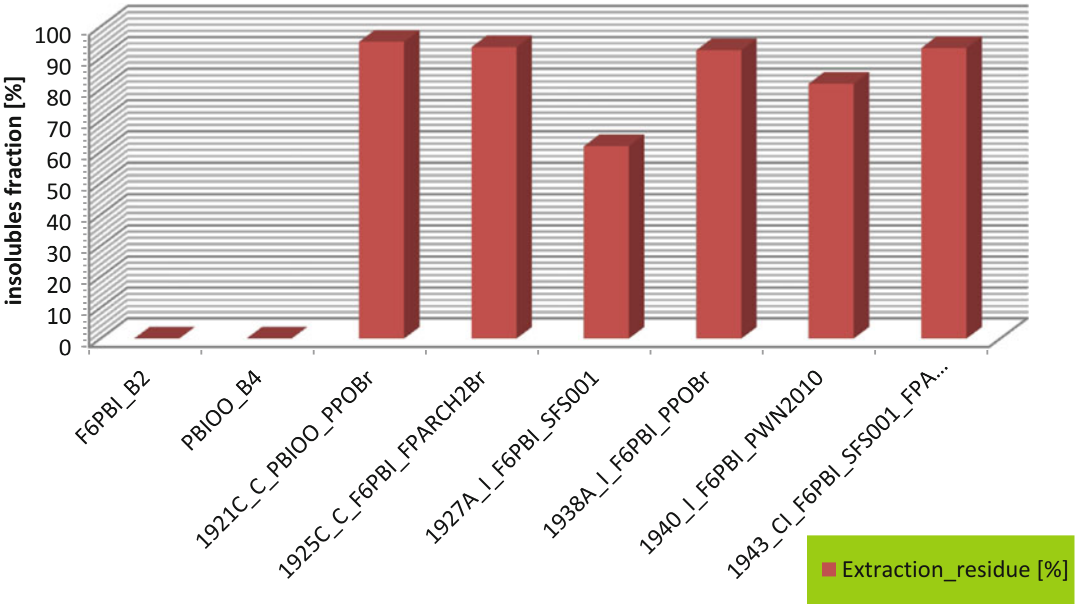

Fig. 4.17 DMAc extraction results of the membranes including the pure membranes F_6PBI (**B2**) and PBIOO (**B4**) (I = ionically cross-linked, C = covalently cross-linked, CI = covalent-ionically cross-linked)

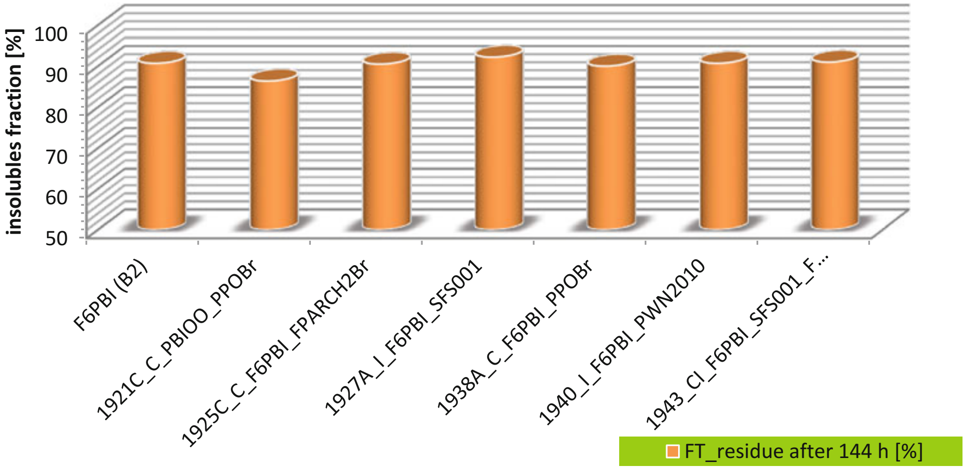

Fig. 4.18 Insoluble residuals of membranes after 144 h of storage in Fenton's Reagent

It can be seen from Fig. 4.18 that all **B2**-containing blend membranes regardless of cross-link type and polymer backbone of the used cross-linkers show very similar weight loss values after the 144 h FT which indicates that **B2** which is known for high oxidative stability as ascertained in the literature reviewed in this chapter (e.g., [49]) determines the excellent oxidative stabilities of those blends. The somewhat higher weight loss value of the **B4**-containing blend membrane (1921A) reflects the worse chemical stability of this polybenzimidazole, compared to **B2** [56]. It must be mentioned here that all membranes retained their mechanical stability after 144 h of FT.

The membranes subjected to FT were further investigated by SEM to see to what extent the membrane surfaces were corroded by the

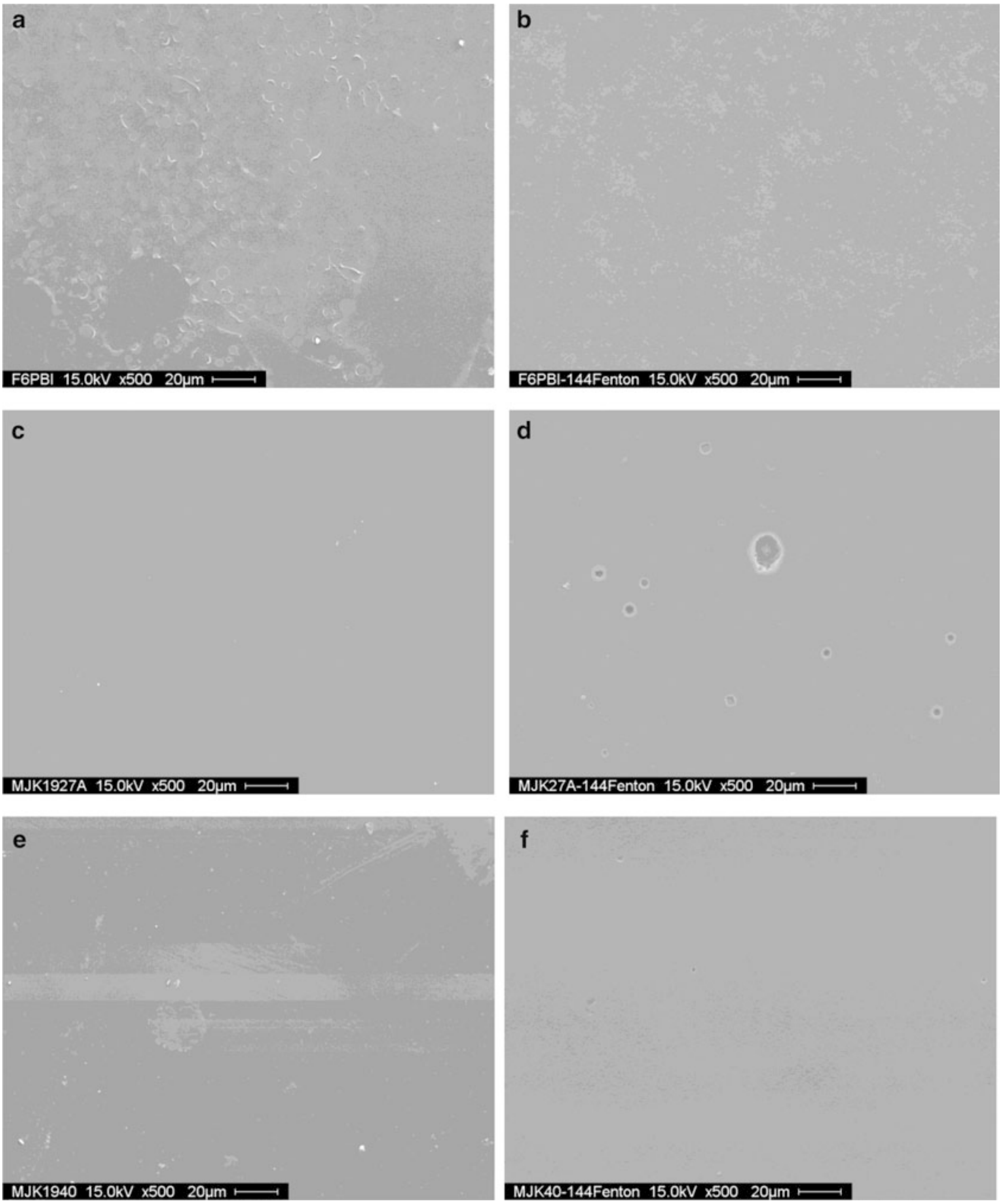

Fig. 4.19 SEM of membranes before and after FT (**a**) **B2** before FT, (**b**) **B2** after FT, (**c**) 1927A before FT, (**d**) 1927A after FT, (**e**) 1940 before FT, (**f**) 1940 after FT, (**g**): 1921C before FT, (**h**) 1921C after FT, (**i**) 1938 before FT, (**j**) 1938 after FT, (**k**) 1925C before FT, (**l**) 1925C after FT. Magnification of all micrographs is ×500

strongly oxidizing Fenton's Solution. In Fig. 4.19, SEM micrographs of the surfaces of the membranes before and after FT are collected.

It is seen from the micrographs that the membrane surfaces exhibit only a few small holes after FT indicating good stabilities of the membranes in the strongly oxidizing FT environment. Only the surface of the membrane 1921C shows more pronounced defects, indicating and confirming the slightly worse chemical stability

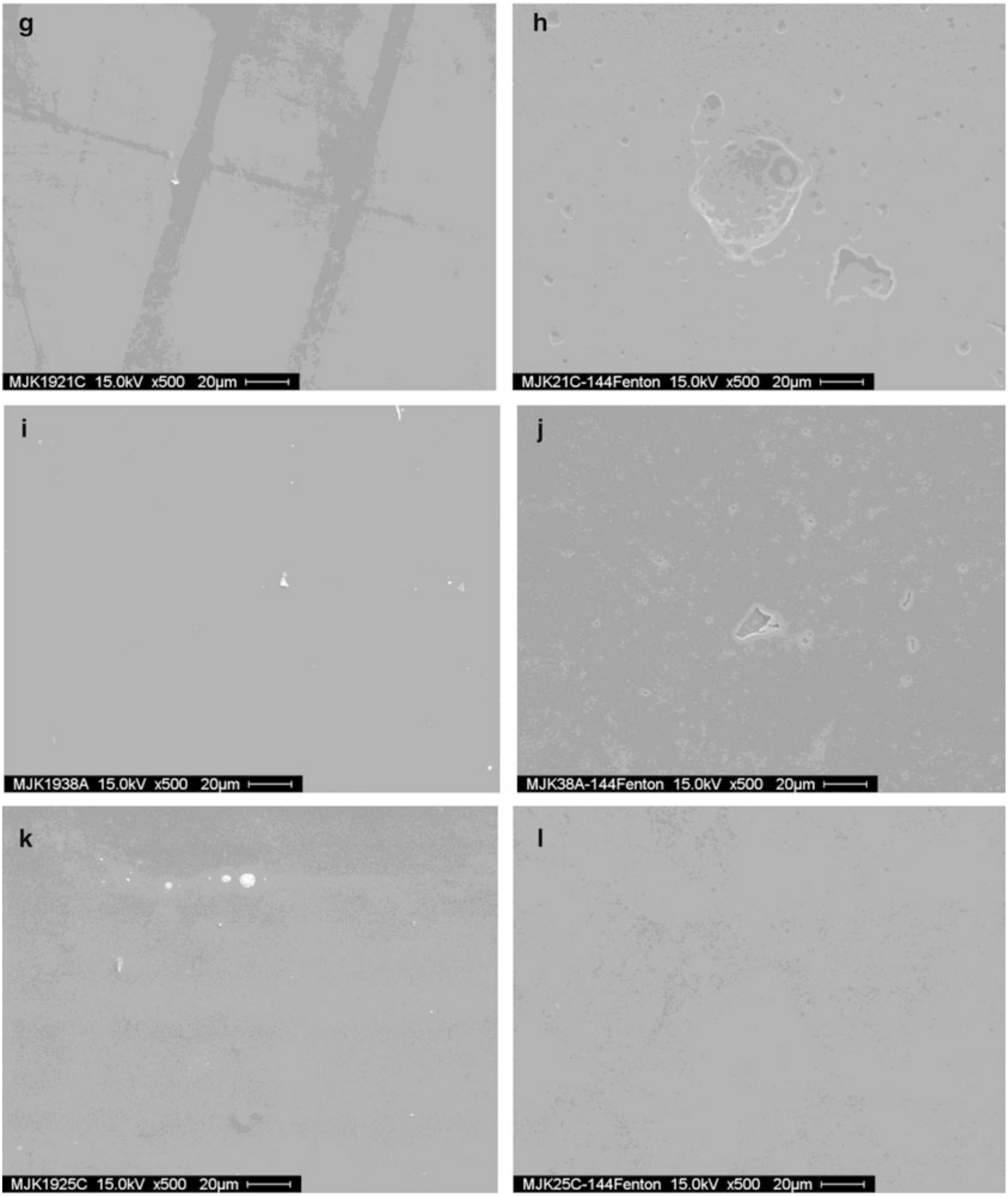

Fig. 4.19 (continued)

of its main blend constituent **B4** as could also be seen from the larger weight loss amount of this membrane after FT (Fig. 4.18), compared to the **B2**-containing membranes. The membranes were also tested via TGA before and after FT to see if the shape of the TGA curve changes through FT which also gives hints for partial chemical degradation of the membranes. In Fig. 4.20, the TGA traces of 1921C before and after FT are presented, and in Fig. 4.21 those of 1938. In both cases, the covalent cross-linking polymer was PPOCH$_2$Br, while the 1921C contains **B4** and 1938 **B2** as polybenzimidazole constituent. It can be seen that the TGA traces of 1921C shows a

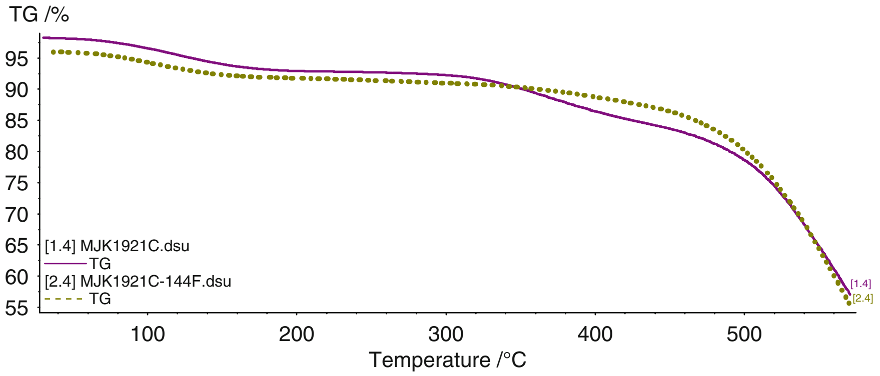

Fig. 4.20 TGA traces of 1921C before and after FT (covalently cross-linked, PPOCH$_2$Br as cross-linker, **B4** as base)

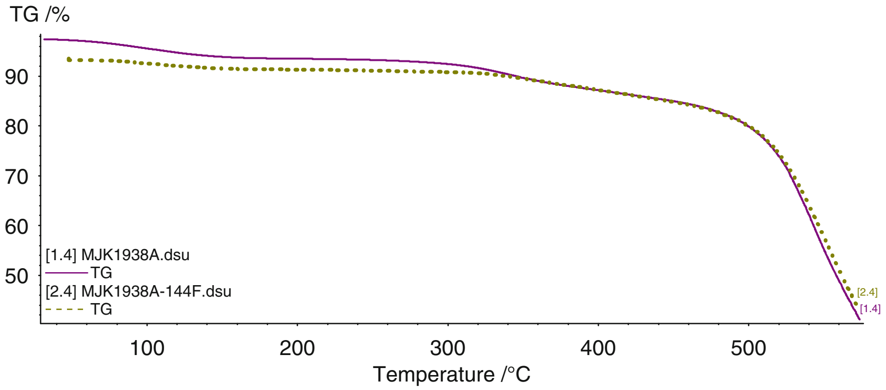

Fig. 4.21 TGA traces of 1938 before and after FT (covalently cross-linked, PPOCH$_2$Br as cross-linker, **B2** as base)

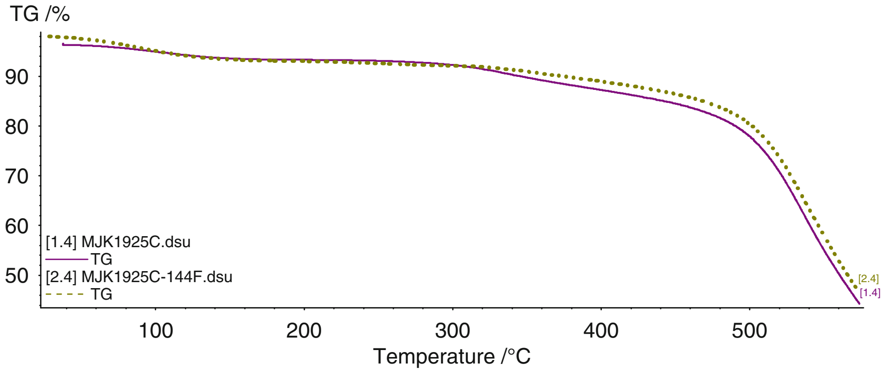

Fig. 4.22 TGA traces of 1925C before and after FT (covalently cross-linked, FPARCH$_2$Br as cross-linker, **B2** as base)

more distinct change of trace shape before and after FT, compared to 1938, which is an indication of stronger chemical changes in the polymer backbones of the 1921C blend components particularly in the *T* range >300 °C in which backbone degradation begins [77]. In Fig. 4.22, the TGA traces of membrane 1925C before and after FT are presented. Both TGA traces of this membrane are nearly identical, reflecting the excellent chemical stability of this membrane. The reason for the

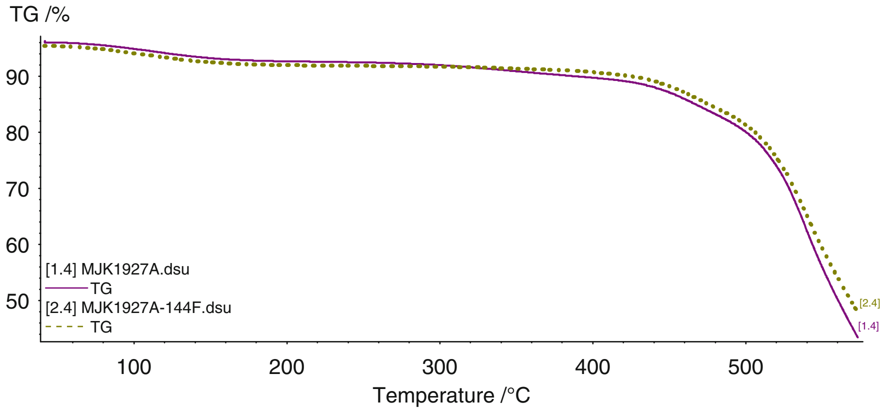

Fig. 4.23 TGA traces of 1927A before and after FT (sulfonated ionical cross-linker **S2**, **B2** as base)

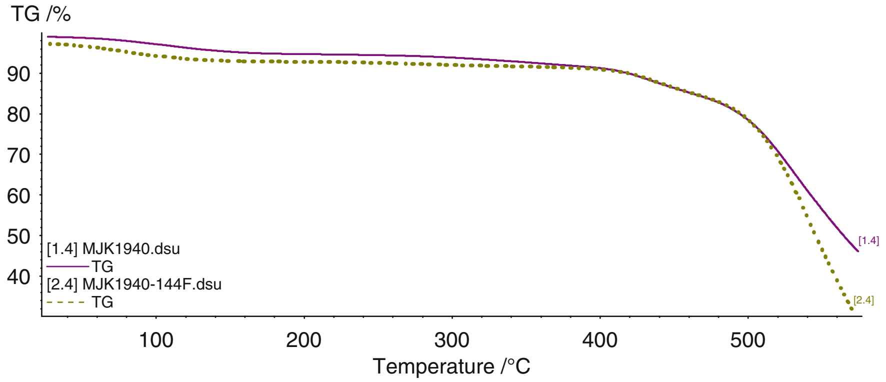

Fig. 4.24 TGA traces of 1940 before and after FT (phosphonated ionical cross-linker **S11**, **B2** as base)

excellent chemical stability of 1925C is most probably that the PPOCH$_2$Br cross-linker was substituted by the chemically more stable cross-linking polymer FPARCH$_2$Br in this membrane.

In Fig. 4.23, the TGA traces of the ionically cross-linked membrane 1927A (sulfonated cross-linker) are presented, and in Fig. 4.24 those of 1940 (phosphonated cross-linker), indicating the excellent chemical stabilities of these two blend membranes.

4.3.3 Proton Conductivity of H$_3$PO$_4$-Doped Membranes

Since the proton conductivity is the determinant property of fuel cell membranes, all membranes of the series were doped with 85 % PA to roughly the same PA doping degree (130 %, ADL = 8.9 in the case of 80 wt% **B2** blends, and ADL = 6.9 in the case of 80 wt% **B4** blends, and ADL = 7.5 in the case of pure **B2**), where possible. Afterwards, the proton conductivity of the membranes was measured under a constant relative humidity of 20 % in a temperature range from 80 to 150 °C. The results of proton conductivity measurements are presented in Fig. 4.25. The proton conductivity measurements were performed with the Membrane Test System (MTS) 740 from Scribner. The method is described in [59].

From Fig. 4.25 no correlation of value of proton conductivity to cross-linking type, F-content or type of cross-linking polymer can be seen: the membrane with the lowest proton

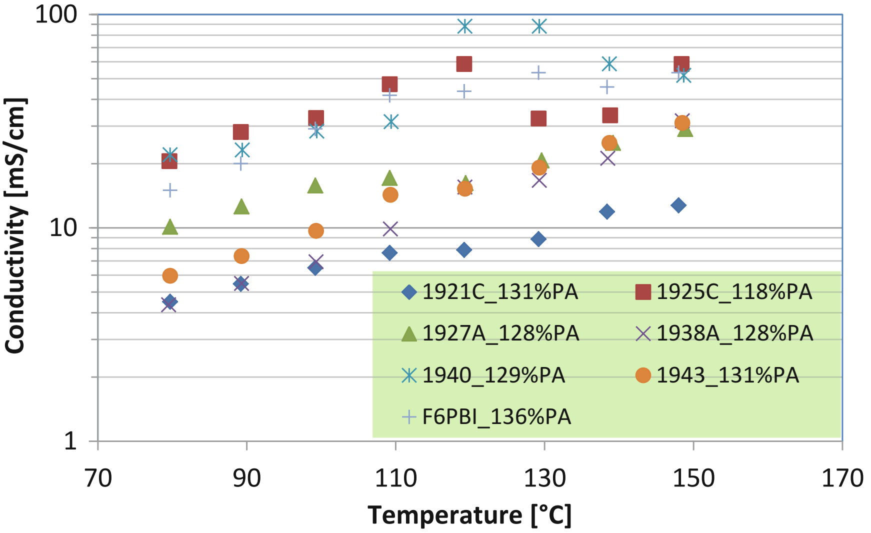

Fig. 4.25 Proton conductivities of the investigated membrane series in dependence of temperature at RH of 20 %

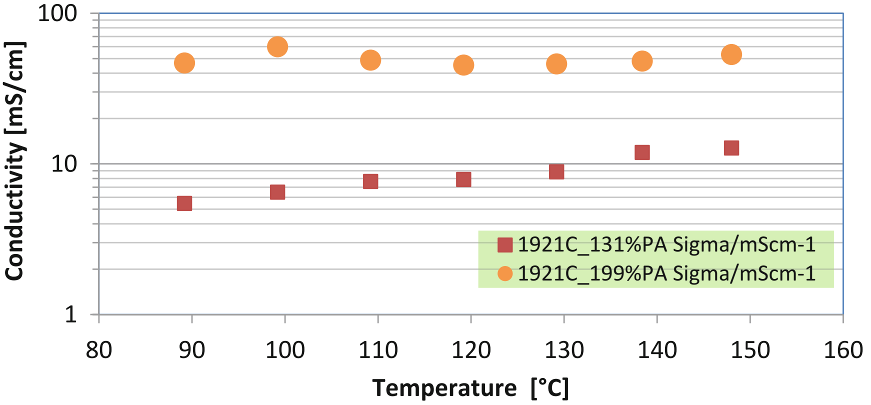

Fig. 4.26 Proton conductivities of the 1921C at 131 and 199 % PA doping degree, respectively, at 20 % RH

conductivities is the covalently cross-linked 1921C containing the nonfluorinated cross-linker $PPOCH_2Br$, while the 1925C, also a covalently cross-linked blend membrane cross-linked with the partially fluorinated $FPARCH_2Br$ polymer, exposes the highest proton conductivity among the investigated membranes. The reason for this finding might be the fact that the relation between structure and properties of the investigated membranes is very complex due to the difficulty of assessability of the influence of the different blend components and cross-linking type on the membrane properties. To elucidate the complex coherence between proton conductivity, PA doping, blend composition, and type of cross-linking of the investigated membranes, a detailed study of the dependence of proton conductivities from relation between the blend components, PA doping degree, temperature, and relative humidities is required. One of the advantages of PA-doped intermediate-T fuel cell membranes is that, if a membrane possesses too low proton conductivities at a specific PA doping degree, the PA doping degree simply has to be increased to obtain a higher H^+ conductivity. This is demonstrated in the membrane 1921C: in Fig. 4.26, the proton conductivities of the 1921C are shown at PA doping degree of 131 % (ADL = 6.96) and 199 % (ADL = 10.57), respectively.

As indicated in Fig. 4.26, with a PA doping degree increase from 131 to 199 %, an increase of proton conductivities of up to a factor of 9 is observed.

4.4 Conclusions

In this chapter, research work done with intermediate-T fuel cell membranes, in which the acid–base blend concept was applied for membrane preparation, was reviewed. The reviewed studies included membranes, where the different parameters have been varied:

- Type of applied polybenzimidazoles
- Type of used ionical cross-linker, including sulfonated and phosphonated ionomers which were either composed of nonfluorinated or partially fluorinated backbones

A mutual characteristic of all the reviewed acid–base blend membrane types are their improved properties compared to pure PBI:

- The mechanical properties of the base-excess acid–base blend membranes are strongly improved, compared to pure PBI.
- The resistance of the acid–base blend membranes to a strongly oxidizing environment (Fenton's Reagent) is markedly enhanced, as indicated by smaller weight losses of the acid–base blend membranes, compared to pure PBI, during storage in Fenton's Reagent.
- The fuel cell performance of the PA-doped base-excess acid–base blend membranes is comparable to that of the best reported pure PA-doped intermediate-T membranes.
- The use of a phosphonated polymer as ionical cross-linker AND proton conductor both in the membrane and the electrodes of intermediate-T MEAs opens perspectives for highly durable intermediate-T fuel cell membranes without PA leaching problems which are always present in PA-doped intermediate-T membranes and MEAs.

When comparing the properties of base-excess blend membranes containing different polybenzimidazoles, it turns out that there is a trend that the use of electron-deficient polybenzimidazoles such as **B2** and **B3** (Fig. 4.4) as basic blend components leads to higher chemical and thermal stabilities of the respective acid–base blend membranes than if more electron-rich PBIs such as **B1** and **B4** are used. However, it must be mentioned here that the molecular weight of the polybenzimidazole also influences the durability of the PBI (blend) membranes: it was observed that after being subjected to FT the membranes lost less weight when their molecular weights were higher [79].

From the reviewed work, it can be concluded that obviously the use of partially fluorinated aromatic cationomers as ionical cross-linkers leads in most cases to better chemical and thermal stabilities of the blend membranes than if nonfluorinated cationomers would be applied as acidic blend components. Among all acidic cross-linkers, the sulfonated and partially fluorinated ionomer **S9** (Fig. 4.5) leads to the best chemical stability of the referring base-excess PBI blend membranes.

From the comparative study covering different ionically, covalently, and covalent-ionically cross-linked PBI blend membrane types, it can be concluded that within the investigated membrane types none of the cross-linking types has principal advantages over the other ones in terms of chemical stability or proton conductivity in PA-doped state.

Future work in the field of PBI blend membranes for use in intermediate-T fuel cells will incorporate:

- Increase of molecular weight of acidic cross-linkers (e.g., of **S9**) to further enhance the chemical, thermal, and mechanical stability of the referring PBI blend membranes
- Investigation of further sulfonated and phosphonated aromatic ionomers as acidic macromolecular cross-linkers (and possibly as proton-conducting blend component) for intermediate-T fuel cell membranes

- Continuation of the R&D work on covalent-ionically cross-linked blend membranes, where the different blend components PBI/acidic polymer/bromomethylated polymer are optimally matched to one another to yield intermediate-T fuel cell membranes with a property profile tailored to the respective membrane application such as fuel cells or electrolysis, respectively
- Electrode and MEA development tailored to the respective intermediate-T membrane(s)

References

1. Grot WG (1994) Perfluorinated ion-exchange polymers and their use in research and industry. Macromol Symp 82:161–172
2. Kreuer KD (1996) Proton conductivity: materials and applications. Chem Mater 8:610–641
3. Vogel H, Marvel CS (1961) Polybenzimidazoles, new thermally stable polymers. J Polym Sci 50:511–539
4. Vogel H, Marvel CS (1963) Polybenzimidazoles 2. J Polym Sci A 1:1531–1541
5. Wainright JS, Wang JT, Savinell RF et al (1995) Acid-doped polybenzimidazoles: a new polymer electrolyte. J Electrochem Soc 142:L121–L123
6. Kreuer KD, Paddison S, Spohr E et al (2004) Toward a new type of anhydrous organic proton conductor based on immobilized imidazole. Chem Rev 104:4637–4678
7. Yu S, Xiao L, Benicewicz BC (2008) Durability studies of PBI-based high temperature PEMFCs. Fuel Cells 8:165–174
8. Liao J, Li QF, Rudbeck HC et al (2011) Oxidative degradation of polybenzimidazole membranes as electrolytes for high temperature proton exchange membrane fuel cells. Fuel Cells 11:745–755
9. Ghosh S, Maity S, Jana T (2011) Polybenzimidazole/silica nanocomposites: organic-inorganic hybrid membranes for PEM fuel cell. J Mater Chem 21:14897–14906
10. Zhang R, Shi ZX, Liu Y et al (2012) Synthesis and characterization of polybenzimidazole–nanodiamond hybrids via in situ polymerization method. J Appl Polym Sci 125:3191–3199
11. Mao L, Mishra AK, Kim NH et al (2012) Poly (2,5-benzimidazole)–silica nanocomposite membranes for high temperature proton exchange membrane fuel cell. J Membr Sci 411–412:91–98
12. Ossiander T, Heinzl C, Gleich S et al (2014) Influence of the size and shape of silica nanoparticles on the properties and degradation of a PBI-based high temperature polymer electrolyte membrane. J Membr Sci 454:12–19
13. Plackett D, Siu A, Li Q et al (2011) High-temperature proton exchange membranes based on polybenzimidazole and clay composites for fuel cells. J Membr Sci 383:78–87
14. He R, Li Q, Xiao G et al (2003) Proton conductivity of phosphoric acid doped polybenzimidazole and its composites with inorganic proton conductors. J Membr Sci 226:169–184
15. Wang S, Zhang G, Han M et al (2011) Novel epoxy-based cross-linked polybenzimidazole for high temperature proton exchange membrane fuel cells. Int J Hydrogen Energy 36:8412–8421
16. Aili D, Li Q, Christensen E et al (2011) Crosslinking of polybenzimidazole membranes by divinylsulfone post-treatment for high-temperature proton exchange membrane fuel cell applications. Polym Int 60:1201–1207
17. Xu HJ, Chen KC, Guo XX et al (2007) Synthesis of hyperbranched polybenzimidazoles and their membrane formation. J Membr Sci 288:255–260
18. Wang KY, Xiao YC, Chung TS (2006) Chemically modified polybenzimidazole nanofiltration membrane for the separation of electrolytes and cephalexin. Chem Eng Sci 61:5807–5817
19. Noyé P, Li QF, Pan C et al (2008) Cross-linked polybenzimidazole membranes for high temperature proton exchange membrane fuel cells with dichloromethyl phosphoric acid as a cross-linker. Polym Adv Technol 19:1270–1275
20. Yang J, Li Q, Cleemann LN et al (2013) Crosslinked hexafluoropropylidene polybenzimidazole membranes with chloromethyl polysulfone for fuel cell applications. Adv Energy Mater 3:622–630
21. Wang S, Zhao C, Ma W et al (2013) Macromolecular cross-linked polybenzimidazole based on bromomethylated poly (aryl ether ketone) with enhanced stability for high temperature fuel cell applications. J Power Sources 243:102–109
22. Cui W, Kerres J (2001) Acid-base polymer blends and their application in membrane processes. US Patent 6,194,474
23. Kerres J, Ullrich A, Häring T (2004) Engineering ionomer blends and engineering ionomer blend membranes. European Patent 1,076,676; US Patent 6,723,757
24. Cui W, Kerres J, Eigenberger G (1998) Development and characterization of ion-exchange polymer blend membranes. Sep Purif Technol 14:145–154
25. Kerres J, Ullrich A, Meier F et al (1999) Synthesis and characterization of novel acid-base polymer blends for the application in membrane fuel cells. Solid State Ionics 125:243–249
26. Kerres J, Ullrich A, Häring T et al (2000) Preparation, characterization, and fuel cell application of new acid-base blend membranes. J New Mater Electrochem Syst 3:229–239

27. Kerres JA (2001) Development of ionomer membranes for fuel cells. J Membr Sci 185:3–27
28. Kerres J, Tang CM, Graf C (2004) Improvement of properties of polyetherketone ionomer membranes by blending and cross-linking. Ind Eng Chem Res 43:4571–4579
29. Kerres J, Xing D, Schönberger F (2006) Comparative investigation of novel PBI blend ionomer membranes from nonfluorinated and partially fluorinated polyarylene ethers. J Polym Sci B Polym Phys 44:2311–2326
30. Hasiotis C, Li Q, Deimede V et al (2001) Development and characterization of acid-doped polybenzimidazole-sulfonated polysulfone blend polymer electrolytes for fuel cells. J Electrochem Soc 148: A513–A519
31. Kawahara M, Rikukawa M, Sanui K (2000) Relationship between absorbed water and proton conductivity in sulfopropylated polybenzimidazole. Polym Adv Technol 11:544–547
32. Pu H, Liu Q (2004) Methanol permeability and proton conductivity of polybenzimidazole and sulfonated polybenzimidazole. Polym Int 53:1512–1516
33. Papadimitriou KD, Andreopoulou AK, Kallitsis JK (2010) Phosphonated fully aromatic polyethers for PEMFCs applications. J Polym Sci A Polym Chem 48:2817–2827
34. Kalamaras I, Daletou MK, Gregoriou VG et al (2011) Sulfonated aromatic polyethers containing pyridine units as electrolytes for high temperature fuel cells. Fuel Cells 11:921–931
35. Thomas OD, Peckham TJ, Thanganathan U et al (2010) Sulfonated polybenzimidazoles: proton conduction and acid-base crosslinking. J Polym Chem A Polym Chem 48:3640–3650
36. Ng F, Peron J, Jones DJ et al (2011) Synthesis of novel proton-conducting highly sulfonated polybenzimidazoles for PEMFC and the effect of the type of bisphenyl bridge on polymer and membrane properties. J Polym Sci A Polym Chem 49:2107–2117
37. Angioni S, Villa DC, Dal Barco S et al (2014) Polysulfonation of PBI-based membranes for HTPEMFCs: a possible way to maintain high proton transport at a low H_3PO_4 doping level. J Mater Chem A 2:663–671
38. Sukumar PR, Wu W, Markova D et al (2007) Functionalized polybenzimidazoles as membrane materials for fuel cells. Macromol Chem Phys 208:2258–2267
39. Gubler L, Kramer D, Belack J et al (2007) Celtec-V, a polybenzimidazole-based membrane for the direct methanol fuel cell. J Electrochem Soc 154:B981–B987
40. Sinigersky V, Budurova D, Penchev H et al (2013) Polybenzimidazole-graft-polyvinylphosphonic acid proton-conducting fuel cell membranes. J Appl Polym Sci 129:1223–1231
41. Ng F, Bae B, Miyatake K et al (2011) Polybenzimidazole block sulfonated poly(arylene ether sulfone) ionomers. Chem Commun 47:8895–8897
42. Hasiotis C, Li Q, Deimede V et al (2001) New polymer electrolytes based on blends of sulfonated polysulfones with polybenzimidazole. Electrochim Acta 46:2401–2406
43. Noshay A, Robeson LM (1976) Sulfonated polysulfone. J Appl Polym Sci 20:1885–1903
44. Xing D, Kerres J (2006) Improved performance of sulfonated polyarylene ethers for proton exchange membrane fuel cells. Polym Adv Technol 17:1–7
45. Takamuku S, Jannasch P (2012) Properties and degradation of hydrocarbon fuel cell membranes: a comparative study of sulfonated poly(arylene ether sulfone)s with different positions of the acid groups. Polym Chem 3:1202–1214
46. Kerres J, Schönberger F, Chromik A et al (2008) Partially fluorinated arylene polyethers and their ternary blend membranes with PBI and H_3PO_4: Part I. Synthesis and characterization of polymers and binary blend membranes. Fuel Cells 8:175–187
47. Walling C (1975) Fenton’s reagent revisited. Acc Chem Res 8:125–131
48. Li Q, Jensen JO, Pan C et al (2008) Partially fluorinated arylene polyethers and their ternary blends with PBI and H_3PO_4: Part II. Characterizations and fuel cell tests of the ternary membranes. Fuel Cells 8:188–199
49. Li QF, Rudbeck HC, Chromik A et al (2010) Properties, degradation and high temperature fuel cell test of different types of PBI and PBI blend membranes. J Membr Sci 347:260–270
50. Henschel C (2006) Membranes and electrodes for fuel cells as PEMEAS merges with E-TEK. Fuel Cells Bull 2:12–15
51. Qi ZQ, Buelte S (2006) Effect of open circuit voltage on performance and degradation of high temperature PBI-H_3PO_4 fuel cells. J Power Sources 161:1126–1132
52. Reiche A (2006) Sartorius HT-PEMFC membrane electrode assembly. Paper presented at the 2006 fuel cell seminar, November 13–17, 2006, Honolulu, Hawaii. http://www.fuelcellseminar.com/pdf/2006/Wednesday/3B/Reiche_Annette_1010_502&507.pdf
53. Stolten D, Wannek C, Dohle H et al (2007) Strategy, status and outlook for HT-PEFC development for APU application. Paper presented at the 2007 fuel cell seminar, October 15–19, 2007, San Antonio, TX. http://www.fuelcellseminar.com/pdf/2007/Presentations/2A/162%20Stolten_San%20Antonio_2007_final.ppt.pdf
54. Kerres J, Ullrich A, Hein M et al (2004) Cross-linked polyaryl blend membranes for polymer electrolyte fuel cells. Fuel Cells 4:105–112
55. Chromik A, Kerres JA (2013) Degradation studies on acid-base blends for both LT and intermediate T fuel cells. Solid State Ionics 252:140–151
56. Liu G, Zhang H, Hu J et al (2006) Studies of performance degradation of a high temperature PEMFC based on H_3PO_4-doped PBI. J Power Sources 162:547–552
57. Steenberg T, Hjuler HA, Terkelsen C et al (2012) Roll-to-roll coated PBI membranes for high

temperature PEM fuel cells. Energy Environ Sci 5:6076–6080
58. Kerres JA, Katzfuß A, Chromik A et al (2014) J Appl Polym Sci 131:39889
59. Hübner G, Roduner E (1999) EPR investigation of HO/radical initiated degradation reactions of sulfonated aromatics as model compounds for fuel cell proton conducting membranes. J Mater Chem 9:409–418
60. Assink RA, Arnold C, Hollandsworth RPJ (1991) Preparation of oxidatively stable cation-exchange membranes by the elimination of tertiary hydrogens. J Membr Sci 56:143–151
61. Ding J, Day M (2006) Novel highly fluorinated poly (arylene ether-1,3,4-oxadiazole)s, their preparation, and sensory properties to fluoride anion. Macromolecules 39:6054–6062
62. Hajdok I, Bona A, Werner HJ et al (2014) Synthesis and characterization of fluorinated and sulfonated poly(arylene ether-1,3,4-oxadiazole) derivatives and their blend membranes. Eur Polym J 52:76–87
63. Sartori P, Bauer G (1978) 2,3,5,6-Tetrafluorbenzoldisulfonsäure aus Pentafluorbenzol-sulfonsäure. J Fluorine Chem 12:203–210
64. Banks RE, Burgess JE, Cheng WM et al (1965) Heterocyclic polyfluoro-compounds. Part IV. - Nucleophilic substitution in pentafluoropyridine: the preparation and properties of some 4-substituted 2,3,5,6-tetrafluoro-pyridines. J Chem Soc (resumed) 1965:575–581
65. Chambers RD, Hutchinson J, Musgrave WKR (1964) Polyfluoroheterocyclic compounds. Part II: Nucleophilic substitution in pentafluoropyridine. J Chem Soc (resumed)1964:3736–3739
66. Alsop DJ, Burdon J, Tatlow JC (1962) Aromatic polyfluorocompounds. Part XI: Some replacement reactions of octafluorotoluene. J Chem Soc (resumed) 1962:1801–1805
67. Seyb C, Kerres J (2013) Novel partially fluorinated sulfonated poly(arylenethioether)s and poly (aryleneether)s prepared from octafluorotoluene and pentafluoropyridine, and their blends with PBI-Celazol. Eur Polym J 49:518–531
68. Seyb C (2014) Synthese und Charakterisierung von teilfluorierten sulfonierten poly(arylen)-Ionomeren für den Einsatz in Mitteltemperaturbrennstoffzellen. Dissertation, Universität Stuttgart
69. Nakano T, Nagaoka T, Kawakami H (2005) Preparation of novel sulfonated block copolyimides for proton conductivity membranes. Polym Adv Technol 16:753–757
70. Iizuka Y, Tanaka M, Kawakami H (2013) Preparation and proton conductivity of phosphoric acid-doped blend membranes composed of sulfonated block copolyimides and polybenzimidazole. Polym Int 62:703–708
71. Einsla ML, Kim YS, Hawley M et al (2008) Toward improved conductivity of sulfonated aromatic proton exchange membranes at low relative humidity. Chem Mater 20:5636–5642
72. Atanasov V, Kerres J (2011) Highly phosphonated polypentafluorostyrene. Macromolecules 44:6416–6423
73. Atanasov V, Gudat D, Ruffmann B et al (2013) Highly phosphonated polypentafluoro-styrene: characterization and blends with polybenzimidazole. Eur Polym J 49:3977–3985
74. Berber MR, Fujigaya T, Sasaki K et al (2011) Remarkably durable high temperature polymer electrolyte fuel cell based on poly(vinylphosphonic acid)-doped polybenzimidazole. Sci Rep 3:1–7
75. Matsumoto K, Fujigaya T, Yanagi H et al (2011) Very high performance alkali anion-exchange membrane fuel cells. Adv Funct Mater 21:1089–1094
76. Galbiati S, Baricci A, Casalegno A et al (2013) Degradation in phosphoric acid doped polymer fuel cells: a 6000 h parametric investigation. Int J Hydrogen Energy 38:6469–6480
77. Papadimitriou KD, Geormezi M, Neophytides SG et al (2013) Covalent cross-linking in phosphoric acid of pyridine based aromatic polyethers bearing side double bonds for use in high temperature polymer electrolyte membrane fuel cells. J Membr Sci 433:1–9
78. Kerres J, Zhang W, Häring T (2004) Covalently cross-linked ionomer (blend) membranes for fuel cells. J New Mater Electrochem Syst 7:299–309
79. Yang JS, Cleemann LN, Steenberg T et al (2014) High molecular weight polybenzimidazole membranes for high temperature PEMFC. Fuel Cells 14:7–15